İSTANBUL BİLGİ UNIVERSITY
INSTITUTE OF GRADUATE PROGRAMS
ELECTRICAL & ELECTRONICS ENGINEERING MASTER
DEGREE PROGRAM

CELL SEPARATION USING MICROCOIL ARRAY INTEGRATED POLYIMIDE AND FR4 PRINTED CIRCUIT BOARD

İpek Hilal KACAR
119815003

Assoc. Prof. Yiğit Dağhan GÖKDEL
Assoc. Prof. Yuk Yin NG

İSTANBUL
2022

CELL SEPARATION USING MICROCOIL ARRAY INTEGRATED POLYIMIDE AND FR4 PRINTED CIRCUIT BOARD

APPROVED BY:

Assoc. Prof. Yiğit Dağhan Gökdel (Thesis Supervisor)	.....
Assist. Prof. Yuk Yin NG	.....
Assist. Prof. Başar Aka	.....
Assist. Prof. Gülsen Betül Aktaş	.....
Assist. Prof. Ceyhun Kırımlı	.....

DATE OF APPROVAL: 07.07.2022

Dedicated to my mother, Ceylan

ACKNOWLEDGEMENTS

I would like to express my gratitude to my supervisor, Assoc. Prof. Yiğit Dağhan Gökdel, for his warm encouragement in a variety of facets of my life, in both my academic and extracurricular endeavors and interests, made it feasible for me to finish my thesis. Also, I would like to express my endless thanks to my friends Beyza Dandin, Can Arda Yıldırım, Arda Güler, Ceren Özcan, Tuğçe Yücel and Can Mert Piker, who contributed as much as I did and supported me in this project. This project could not have been completed without them, they have all become people whom I trust very closely, rather than just being a laboratory member, on this path we move forward by motivating each other. I am very grateful to my laboratory friends Kuter Erdil, Berkay Alçiçek, Gökalp Akcan, Ayşin Arseven and Berfin Gedlac, who have always supported me with their love and friendship. I know that the support of Yiğit Özdinç, Ecem Önen, Efe Tangüner, Kardelen Olcay and İrem Tatlıcı cannot be denied, whom I see as my brothers and sisters in my life, and I feel very lucky to have them in my life. Even though I was an only child, I never felt the lack of siblings thanks to you. My parents Ceylan and Galip Kacar have taught me so much and have given me more than I could ever hope for. I am eternally grateful to them. Finally I dedicate this thesis to my mother, Ceylan, whom I lost very early and unexpectedly. I wouldn't be here today without your love and guidance. The memories we shared together still brings color and joy to my life as I remember them. You were not only a mother to me but you were also my friend, I want to believe that somehow you see the things I do because I regret that I can't share them with you. I hope that one day our paths will cross again in another universe. You were and will remain my Patronus Spell.

"From the tip of his wand burst the silver doe. She landed on the office floor, bounded once across the office, and soared out of the window. Dumbledore watched her fly away, and as her silvery glow faded he turned back to Snape, and his eyes were full of tears. "After all this time?" "Always," said Snape."

ABSTRACT

In this thesis, a cell separation system using planar coil arrays is proposed with double layered PCBs. The system has been designed, fabricated, and tested as an alternative method for magnetic cell isolation. Here it is not aimed to propose a highly effective and sensitive standard cell separation device, but we have presented a cheap, less harmful, and sufficiently sensitive device with a novel method. Within this thesis, we proposed FR4 (Rigid) and Polyimide (Flexible) based, easy and quick-to-fabricate, printed circuit board having double layered different sized planar coils to measure the total magnetic field output. In this work, the working principles of a simple magnetic cell separator is improved using this proposed magnetic cell separation methodology. Also, the sensitivity of planar coil printed circuit boards, which are used old-fashioned and unrepeatable fabrication methods is enhanced. Our work does not aim to separate cells high-sensitively, but it proposes a novel method which decreases damage of the cells. The planar coil size that gets optimum efficiency is selected by checking the planar coil tests performed. By using square planar coils of different sizes and turns, first the values to optimize the planar coil design were found, and then the magnetic field comparison was made by printing on two different substrates as FR4 and polyimide. After the overheating problem of the circuit was resolved, the damage to the cells approached almost zero. Our work does not aim to separate cells high-sensitively, but it proposes a novel and more advanced version of cell isolation process. Although cell separation does not contain 100% purity, our project has made it a preferable system since it is a perfectible method by converting it into a flexible structure. As can be seen in the Experimental Results Chapter, the results obtained were successful and a successful alternative method to the traditional method could be proposed.

ÖZET

Bu tezde, çift katmanlı PCB'ler ile düzlemsel bobin dizileri kullanan bir hücre ayırma sistemi önerilmiştir. Sistem, manyetik hücre izolasyonu için alternatif bir yöntem olarak tasarlanmış, üretilmiş ve test edilmiştir. Burada oldukça etkili ve hassas bir standart hücre ayırma cihazı önermek amaçlanmamıştır, ancak yeni bir yöntemle ucuz, daha az zararlı ve yeterince hassas bir cihaz sunulmuştur. Bu tez kapsamında, toplam manyetik alan çıktısını ölçmek için FR4 (Rijit) ve Poliimid (Esnek) bazlı, kolay ve hızlı üretilebilen, çift katmanlı farklı boyutta düzlemsel bobinlere sahip baskılı devre kartı önerilmiştir. Önerilen bu manyetik hücre ayırma metodolojisi kullanılarak basit bir manyetik hücre ayırıcının çalışma prensipleri geliştirilmiştir. Ayrıca geleneksel ve tekrarı olmayan fabrikasyon yöntemlerinin kullanıldığı düzlemsel bobin baskılı devre kartlarının hassasiyeti artırılmıştır. Çalışmamız hücreleri yüksek hassasiyetle ayırmayı amaçlamamakta, hücrelerin hasarını azaltan yeni bir yöntem önermektedir. Yapılan düzlemsel bobin testleri kontrol edilerek optimum verim sağlayan düzlemsel bobin boyutu seçilmiştir. Farklı ebat ve dönüşlerde kare düzlemsel bobinler kullanılarak öncelikle düzlemsel bobin tasarımını optimize edecek değerler bulunmuş, ardından FR4 ve poliimid olmak üzere iki farklı alt tabakaya baskı yapılarak manyetik alan karşılaştırması yapılmıştır. Elde edilen sonuçlara göre geleneksel yönteme göre daha yavaş olmasına rağmen %20 daha az zararlı bir yapı geliştirilmiştir. Devrenin aşırı ısınma sorunu çözüldükten sonra hücrelere verilen hasar neredeyse sıfıra yaklaşmıştır. Hücre seçimi %100 saflık içermese de canlı hücrelere daha az zararlı olduğu için projemiz onu tercih edilen bir sistem haline getirmiştir. Aynı zamanda esnek bir yapıya dönüştürülebilmesi ve içindeki hücrelerin tüpün çevresinden manipüle edilebilmesi, geleneksel tek taraflı hücre ayırma yöntemlerine göre oldukça yenilikçi bir yaklaşımdır. Deneysel Sonuçlar Bölümünde görüldüğü gibi, elde edilen sonuçlar başarılı olmuş ve geleneksel yönteme başarılı bir alternatif yöntem olarak önerilebilir haldedir.

TABLE OF CONTENTS

LIST OF FIGURES

LIST OF TABLES

1. INTRODUCTION

Cell separation is at the heart of today's experimental biology and medical procedures. Its significance is shown by physical and biological concepts that have been investigated for use in cell separation. Both clinical and fundamental biology research rely on cell isolation. Isolating a subpopulation of cells from a broad, diversified population allows for the enrichment of a specific population, revealing the isolated population for further investigation.

The necessities of biological and medical research, as well as the ever-increasing demands for sensitivity, selectivity, yield, timeliness, and process economy, are driving the development of cell separation technologies [2]. The capacity to sort cells into discrete populations allows researchers to analyze particular cell types isolated from a diverse starting population with little (or no) contamination from other cell types [3]. Many breakthroughs in cell biology have been made possible by this technique, which is also allowing study in fields as diverse as regenerative medicine, cancer treatment, and HIV pathogenesis. Experiments on isolated cells allow scientists to confidently answer specific research questions since other cell types in the sample are minimized [2, 4].

For sample preparation in many biological experiments, such as disease detection, rare cells must be separated and concentrated. Devices have emerged as a viable platform for cell sorting applications because to a number of benefits, such as their compact size, low cost, minimal sample and reagent consumption, mobility, and short analysis time [3]. There are three methodologies of cell separation.

Principle	**Advantages**	**Disadvantages**
Adherence	Fast, inexpensive, high purity, no need for a specific marker	Low purity, can be harmful to cells
Density	Simple, fast, inexpensive, more than two types of cells can be isolated simultaneously, no need for a specific marker	Low purity, can be harmful to cells
Antibody	Simple, quick, and reasonably priced, high purity, not harmful, high throughput, separation of rare cell populations	Restricted to surface indicators, reliant on the accessibility of antibodies, one marker can only be used to label cells at a time.

Table 1.1: Advantages and disadvantages of three methodologies of cell separation.

Cell separation methods are currently commercially accessible in a wide range of formats, although they are primarily based on these three methodologies [5]:

1) Adherence Target cells is also distinguished from heterogeneous populations using the distinctive adhesion characteristics of assorted cell types. Adherent cells is distinguished from cells in suspension by selecting the correct growth factors and cell culture plates to encourage or hinder adherence.

Due to their innate adhesion properties, macrophages frequently become separated from peripheral blood and bone marrow [6]. The macrophages will be separated once the supernatant containing undesirable cells is removed.

2) Density

Based on the density range of the gradient fluid and sample particles, density gradient centrifugation separates particular cell populations of biological particles. In order to separate the cells within the sample into discrete layers, density-based cell separation often incorporate spinning the sample in a centrifuge in an exceedingly circular motion at the correct angular velocity [2]. Denser cells are pulled away from the axis of rotation by the centripetal acceleration [5]. The less dense cells are displaced during this process by the denser ones [5].

The outcome is that the least dense cells are shifted to be close to the top of the container and the densest cells are pressed to the bottom.

3) Antibody binding

Within this thesis, the focus is on magnetic cell separation. Magnetic cell separation, also known as immunomagnetic cell separation or magnetic cell sorting, involves utilizing antibodies or ligands directed against specific cell surface antigens to target cells for selection or depletion [3].

Magnetic particles, commonly known as magnetic beads, are cross-linked to labeled cells and can be immobilized when an magnetic field is applied [7]. Magnetic cell separation is one of the most widely used procedures for isolating highly pure populations of certain cell subsets due to its speed and simplicity [7].

1.1. Traditional Magnetic Cell Separation Method

To enrich a certain cell type from a mixed population, scientists utilize magnetic activated cell isolation, commonly known as macs cell sorting or macs cell separation [8]. Cell selection or isolation in order to research of a single cell type utilizes this method.

The technique was created using the MACS system from Miltenyi Biotec, which makes use of nano-magnetic beads and columns [8]. The magnetic beads are around 100 nm in size [9]. To capture the targeted cells inside the column, they're employed to tag the particular cells. The column is sandwiched between two permanent magnets, allowing the tagged cells to be caught when the magnetic particle-cell combination travels through it. When the column is positioned between the permanent magnets, the field of magnetic force increased to fasten the separation effectiveness.

This thesis offers a design for cell manipulation, basically, it provides a new structure for the distinction of a magnetically polarized cell. The traditional method used in magnetic cell separation is to use a large permanent magnet. Due to the disadvantages of using magnets; smaller, portable and flexible coils that can create an arbitrary magnetic field is preferred in the thesis.

The aim is to mark and extract cells with a magnetic field that is intended to be generated through planar coils which are tiny electrical conductors. Induction-based circuit designs have the significant advantage of being particularly suitable for operation in adverse settings, such as damp or unclean surroundings

The problem with traditional methods is when a permanent magnet is used, some cells are getting damaged during the separation process pulled the cells very quickly by a large magnetic field. In this thesis we aim to prevent damage to cells by creating less and sufficient magnetic field. In addition, it is one of the goals of the thesis to create a helical domain and improve manipulation of cells by creating a system that actuates a coil filled matrix at any given time. [10]

2. RELATED WORKS

2.1. Magnetic Cell Separation

A ferrous iron-oxide core is surrounded by a polymer shell, or a magnetic 'pigment' incorporated in a polymer matrix, in the magnetic beads themselves.

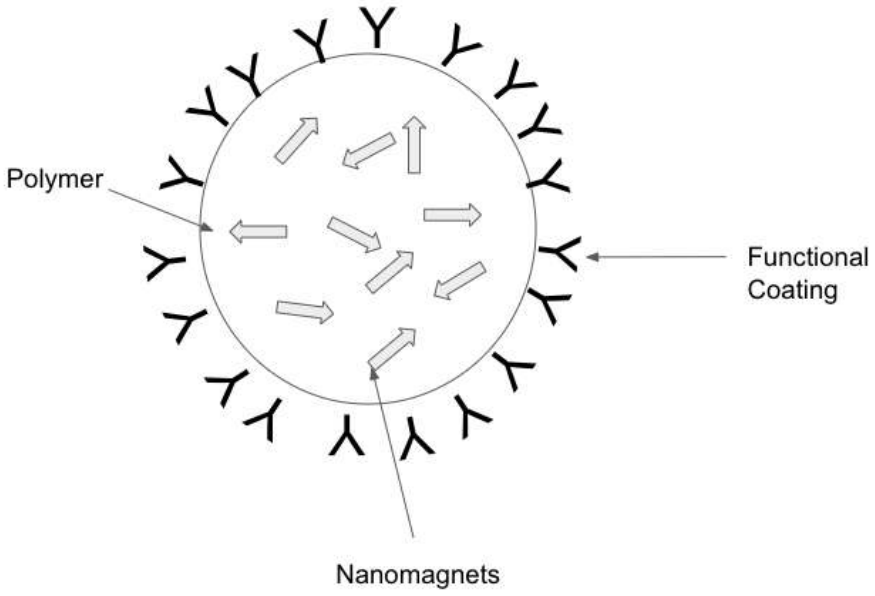

Figure 2.1: Inner structure of a magnetic bead with B = 0

The beads' behavior in a magnetic field is influenced by their size [11]. If the beads are tiny enough, they will be paramagnetic, which means that under a zero magnetic field, they will have no permanent magnetism. Basically, unlike a refrigerator magnet, when an external magnetic field is added and withdrawn, these small paramagnetic beads get magnetized and demagnetized quickly [3, 12, 13]. This has the tremendous benefit of allowing magnetic bead cell separation to be done in a single vessel without the need of a centrifuge or disposable columns [13]. The size of magnetic beads varies from a few nanometers to a few micrometers. The size of magnetic beads affects their behavior.

Sizes of conventional magnetic beads are greater than 1000 nm. At order to improve the surface area of the beads, newer beads are being created in increasingly smaller sizes (down to a few hundred nanometers). As a result, the binding capacity is raised. The beads precipitate more quickly the bigger they are. During magnetic cell separation, magnetic beads, are spherical, have a narrower size distribution, and form cooperative chains [11]. As a result, magnetic beads behave more predictably during magnetic bead cell isolation, reducing separation time dramatically [13].

Positive and negative magnetic cell separation are the two forms of magnetic cell separation. The target cell is recognized and conjugated using positive separation procedures.

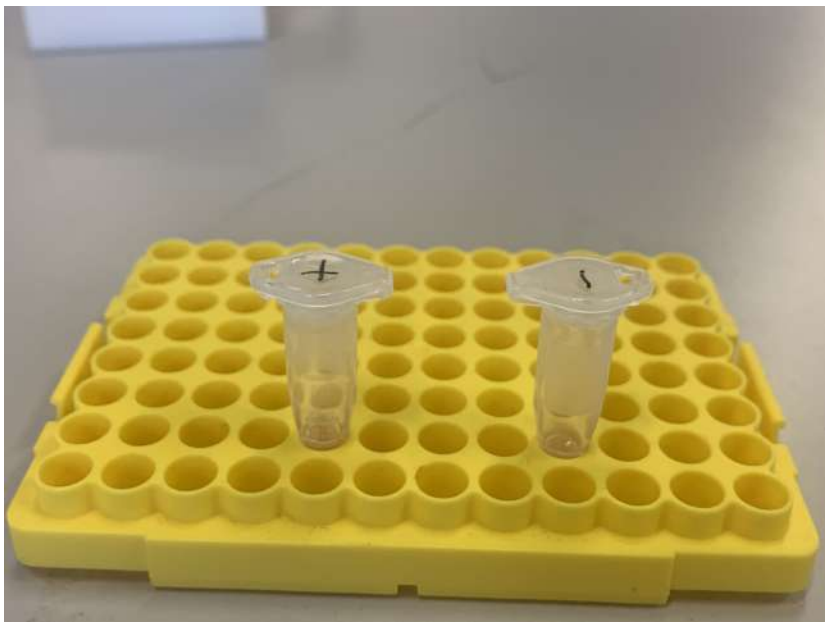

Figure 2.2: Positively and negatively marked cell solutions.

Positive Selection	**Negative Selection**
Isolated cells are extremely pure.	Isolated cells aren't always as pure as they appear.
Antibodies and magnetic particles are commonly used to bind isolated cells.	Magnetic particles do not bind isolated cells.
The antibody cocktail is designed to attack a specific surface marking on the target cells.	With minimum sample manipulation, protocols are quicker and easy to follow.
It is possible to extract additional cell populations from the negative fraction.	All undesired cells are targeted by the antibody cocktail, while desired ones are not.

Table 2.1: Properties of Positive and Negative Selection of Cells.

A magnetic separator isolates and retains those targets near the container's borders, while the remainder undesirable cell solution is withdrawn and replaced with a new buffer. The magnetic beads are functionalized in negative selection to detect the undesirable cells. These are then magnetically separated from the solution, and the remaining targets are decanted and kept [9, 14]. The target cells are not coupled to the magnetic beads at any stage throughout the procedure, which is one advantage of negative selection. Negative selection, on the other hand, may lack the precision of positive selection and necessitate numerous separation processes.

For this reason, considering the advantages of both methods, in this thesis, both negative and positive magnetic cell separation methods are compared with each other. And since it has been tried with both methods, the results are guaranteed.

2.2. Planar Electromagnetic Coil Inductor

Induction-based devices have the significant benefit of being particularly appropriate for operation in adverse settings, such as damp or unclean surroundings, as compared to other types of lab on chip devices [15]. A planar-coil inductor has a closed magnetic circuit [16]. The planar-coil inductor's conductor is designed on a twi dimensioned plane to prevent conductor disconnections. High electromagnetic qualities become increasingly harder to attain as the device's size lowers [17].

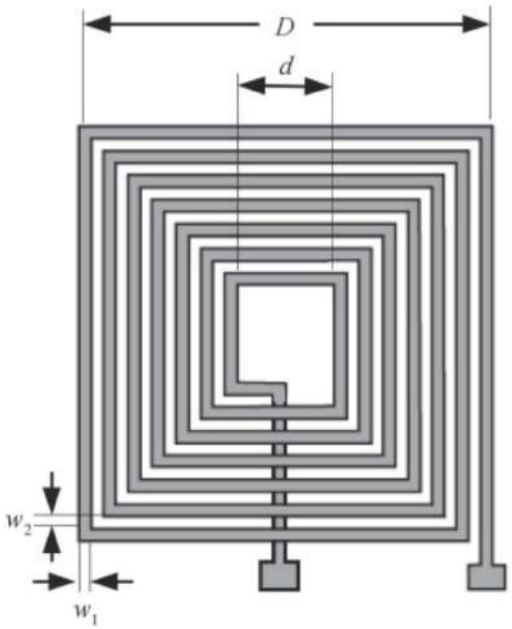

Figure 2.3: The layout of a rectangular planar spiral coil and its dimensional design parameters.

When space is restricted, coils are an excellent alternative for inductive coupling. When two conductors are set up so that a change in current through one wire generates a voltage across the ends of the other wire by electromagnetic induction, this is referred to as being inductively or magnetically connected. In actuality, planar inductors (coils) on the MEMS scale generally have a small number of turns (often fewer than 50) and self inductance values in the hundreds of nH range. Increasing the turn density of planar coils while maintaining the conductor section big enough to prevent ohmic losses and Joule heating is a technological critical point [18].

These coils may be produced on both rigid and nonrigid surfaces, allowing them to be incorporated into both printed circuit boards and flex circuits [19]. Furthermore, because planar coils can be printed on traditional circuit boards (PCB) or flexible materials, they can be produced in a highly reproducible, predictable, and cost-effective manner, making assembly and integration processes easier.

The internal area of a planar coil is dependent on its outer diameter, the number of turns, the width of the wire, and the space between turns [20]. Because inductance is proportional to the magnetic field energy stored by a coil when one unit of electric current flows through it, changes in magnetic field density (B) and distribution caused by bending or folding can help explain inductance variance [21]. Spiral coils are now the most widely used, however they have low fundamental magnetic flux heights. The distance between the centers of the two coils is less than the space between the coils, reducing the distance of electrical energy transfer and the capacity to resist deflection. Square coils provide a more homogeneous magnetic field on and around the surface than circular coils, despite the fact that circular coils produce a greater magnetic field [22].

The structure of one induction coil is shown in Fig. 3.2, which is a planar square spiral coil. Its dimensional design parameters are [23]:

- N, number of turns.
- D, longer outermost side length.
- d, shorter outermost side length.
- w_1, gap or spacing between turns.
- w_2, conductor width.

The two terminal of induction coil are elicited from different sides of the thin film, which are connected via a hole locates on the coil center. Also the induction coil can be designed to be two layers, which can double the number of turns.

D	Total Inductance	d	Conductor & Gap Width	Turns per Layer (N)
12 mm	26.72 μH	0.8 mm	0.08 mm	35
10 mm	15.508 μH	0.72 mm	0.08 mm	29
8 mm	7.952 μH	0.64 mm	0.08 mm	23
6 mm	3.296 μH	0.88 mm	0.08 mm	16
4 mm	0.912 μH	0.8 mm	0.08 mm	10

Table 2.2: The layout of a rectangular planar spiral coil and its dimensional design parameters.

Table 2.2 shows the different sizes and parameters of printed square coils. Magnetic field tests were carried out by choosing 5 different size scales, especially considering the number of turns. The experimented results and continuation of the subject will be discussed under Chapter 4.

2.2.1. Magnetic Field Distribution of Square Spiral Coil

A magnetic field is actually a form of energy that has been stored. The distribution of this energy is represented by the physical distribution of the magnetic field [24]. Understanding the magnetic field's qualities exposes not only the amount and position of stored energy, but also how and where this energy is connected to other electrical circuit elements [24].

The magnetic field distribution on the coil surface must be studied and then he magnetic field strength created by the square coil should be calculated. A magnetic field created by a straight current carrying wire at a point P in space, according to Biot-law [25, 26], Savar's is as indicated in Equation (1). A four-segment current-carrying straight wire can be utilized for each straight wire in a single-turn square coil [16]. The general formulation of the magnetic field distribution of the square coil may be obtained by calculation and vector superposition [27].

$$B = \frac{\mu_0 I}{4\pi d} \times \cos\theta_1 - \cos\cos\theta_2 \tag{2.1}$$

$\mu_0 = 4\pi \times 10^{-7} N \cdot A^{-2}$ is the vacuum permeability, I is the current intensity, and d is the distance from point P to the wire in the formula (2.5). The angle between the wire's ends and the point P is $\theta_{1,2}$. The formula may be used to solve the magnetic field distribution of the square coil (2.5).

3. PROPOSED SYSTEM

The system proposed within this thesis is illustrated in Figure 3.1 which shows a double-layer rigid FR4 planar coil PCB. Planar coils are operated by placing them on both sides of the tube. In this process, the coils in the planar coil arrays are operated to create a magnetic field.

While permenant magnet is used in the traditional method, FR4 planar coils are used in this thesis. Traditionally the permanent magnet is placed on one side, in this thesis, the planar coil circuits are placed on both sides to create a bidirectional magnetic field. Polyimide and FR4 substrates were used in order to experiment two methods in different approach.

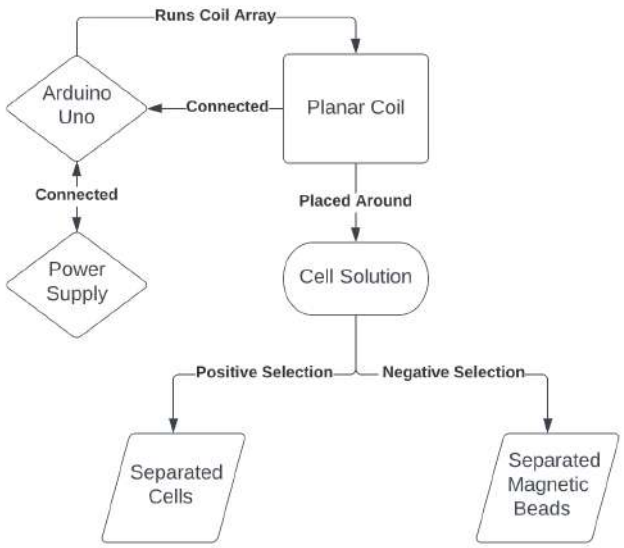

Figure 3.1: Diagram of the Proposed System.

Polyimide material was used specifically because of it's flexibility, a non-rigid PCB was created with a bendable structure to place the planar coils around the tube, thus creating a more effective attraction area [28, 29]. On the other hand, FR4 was used as it can be seen from the tested results (see chapter 6) that more durable results are obtained when working with high current.

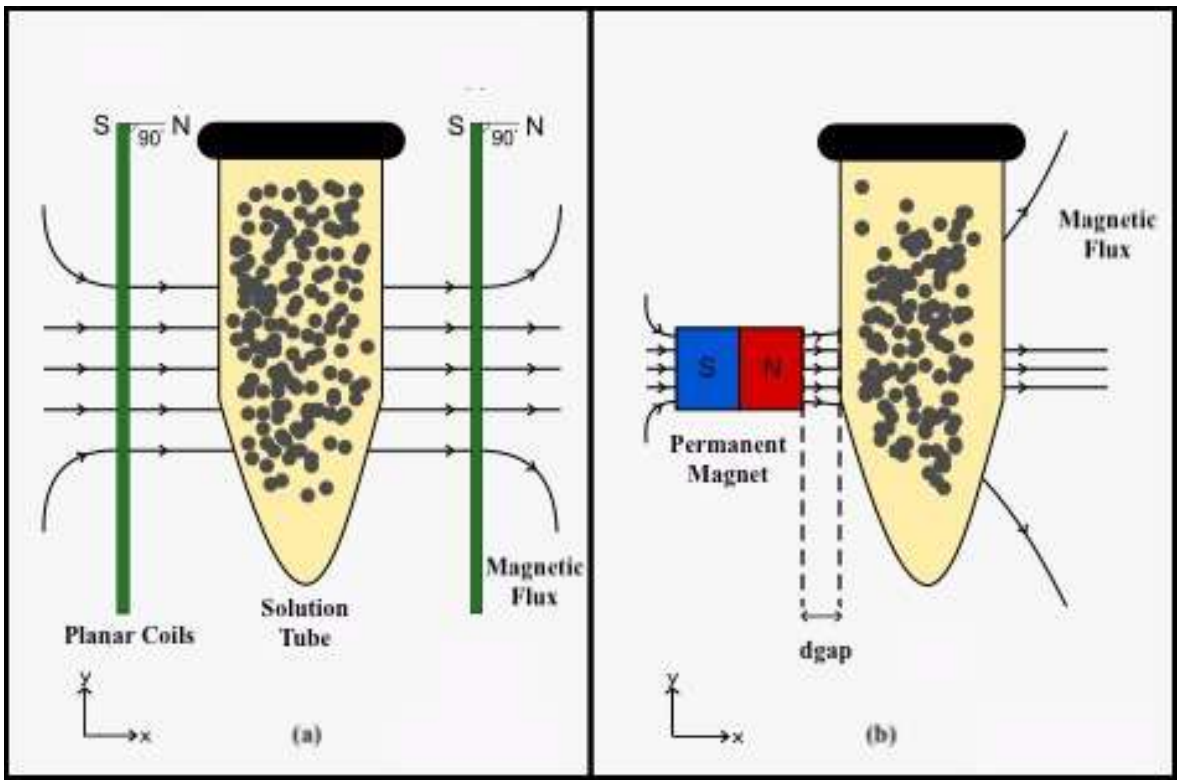

Figure 3.2: Proposed system design compared to conventional design, (a) Proposed design with 2 FR4 planar coil PCBs, (b) Conventional cell separation method using permanent magnets where dgap = 0.

FR4 plates were placed to the sides of the tube instead of wrapping around [30]. By using these two different materials, both their durability was measured and the first steps were taken for the flexible version of this project in future research. This design aims to create more magnetic fields by using smaller coils compared to older designs. In addition, a slower and calmer process is aimed to increase the viability of cells damaged by excessive magnetic field. Since polyimide is a flexible material, its suitability has been tested to prepare a structure that can be wrapped around the tube in future works of the project.

Research with polyimide is still in the testing phase and has only been tested with a coil with 35 turns and 12 mm outer diameter. In the proposed system, planar coils are connected to each other as an array and are controlled by a driver circuit. By using a microcontroller, planar coils in the array are driven so that they can operate. Current and voltage values are variable, thus can be changed by feeding the circuit

with the power supply.

4. PROPOSED DESIGN

The design approaches employed for the project are given in this chapter, as superficially indicated in Chapter 3. These notions were created to offer useful information that may be utilized to improve the design of planar coils and the printed circuit board.

Section 4.1 discusses the design of the planar coils according to the restrictions of the fabrication procedures, as well as their inductive characteristics and various planar coil sizes are evaluated to determine their capabilities. Section 4.2 explains how the FR4 and Polyimide materials structure's differentiate. Suggested printed circuit board design is elaborated with its design parameters in Section 4.3. In Section 4.4, three dimension (3D) design that is planned to hold the whole system together is discussed and the limitations of its construction are argued.

4.1. Planar Coil Design

The goal of this study is to learn more about inductive planar coil and develop them. This chapter seeks to give background information on planar coils, including design considerations and production processes, as well as the evolution of planar coil design over time. Many techniques and modeling approaches used to characterize and predict the characteristics and performance of various planar coils are discussed.

Many factors influence the design of a planar coil and its performance. Design restrictions are frequently concentrated on the manufacturing limits, as well as additional application-specific constraints like as size and inductance [23].

When designing a planar coil, there are six parameters to consider. The number of turns, turn width, turn spacing, average outer and inner diameter, and fill ration are all factors to consider [31]. Total trace length should be raised, number of turns increased, turn width lowered, spacing between turns decreased, average diameter increased, and fill ration decreased to improve inductance [23, 31]. The turn width should raised, and turn spacing decreased to reduce resistance and therefore enhance the Q factor [32].

D	Total Inductance	d	Conductor & Gap Width	Turns per Layer (N)
12 mm	26.72 μH	0.8 mm	0.08 mm	35
10 mm	15.508 μH	0.72 mm	0.08 mm	29
8 mm	7.952 μH	0.64 mm	0.08 mm	23
6 mm	3.296 μH	0.88 mm	0.08 mm	16
4 mm	0.912 μH	0.8 mm	0.08 mm	10

Table 4.1: The layout of a rectangular planar spiral coil and its dimensional design parameters.

Table 4.1 shows the different sizes and parameters of printed square coils. Magnetic field tests were carried out by choosing 5 different size scales, especially considering the number of turns, continuation of the subject will be discussed under Chapter 7.

Two specified qualities are crucial to consider when building planar coils: inductance and resistance. The resistance should be as low as possible (0 is optimal), as any resistance reduces the coil's performance [33]. The inductance, on the other hand, should be large in order for the device to be connected to another system. Inductance is a concept in electrical circuit design that allows to predict and quantify the effects of magnetically stored energy in the circuit [24].The design is optimized and forecasted the magnitude of parasitic circuit elements by applying the basic concepts of magnetic field behavior to planar magnetic coils [32, 33].

The magnetic field is created by the current flowing through the coil, and the inductance is determined by the ratio of current to field. Because the copper coil is thin (0.08 mm thick with a width and height of 0.16 mm), modeling it as a boundary rather than a portion with volume makes sense. In particular, planar coils in 3 different sizes were compared and the coil that gave the most optimal values was selected.

Output Parameters	A
Name	Output
Total inductance - Square	7.773 µH
Sensor frequency	5597.695 kHz
Q factor	50.37
AC resistance (skin effect only)	5.428 Ω
Coil fill ratio	0.15
Coil inner diameter (D_{in})	1.8 mm
DC resistance	3.088 Ω
Average diameter	6.9 mm
Geometric mean diameter	0.739
Self inductance per layer	1.963 µH
Coil length per layer	469.2 mm
Skin depth	0.028 mm
Self resonant frequency	28.543 MHz
Resonance impedance	14321.195 Ω
Current	0.099 mA
Power dissipation	0.178 mW

Output Parameters	B
Name	Output
Total inductance - Square	4.439 µH
Sensor frequency	7431.561 kHz
Q factor	51.187
AC resistance (skin effect only)	4.049 Ω
Coil fill ratio	0.16
Coil inner diameter (D_{in})	1.6 mm
DC resistance	2.138 Ω
Average diameter	5.8 mm
Geometric mean diameter	0.724
Self inductance per layer	1.133 µH
Coil length per layer	324.8 mm
Skin depth	0.024 mm
Self resonant frequency	41.377 MHz
Resonance impedance	10962.229 Ω
Current	0.129 mA
Power dissipation	0.232 mW

Table 4.2: More detailed design parameters of the most efficient planar coils. A shows 29 turned planar coil with 10 millimeters while B shows 35 turned planar coil with diameter of 12 millimeters.

4.2. Machine Design

According to the tube dimensions and shape, a holder is also designed to keep the system standing. Since planar coils are used instead of permanent magnets used in the traditional method, a system that can hold them was needed. Based on the separation racks in the old method, a structure such as a sleeve has been developed in which the tubes can be put in and the coil circuits can sit around. It is designed based on the dimensions of Eppendorf tubes and planar coils. Conventional magnetic cell separation system is referenced and it is optimally adapted for the new system. Since the planar coils are small and difficult to spread the magnetic field, they are designed in such a way that there is zero distance between the tube and the PCB.

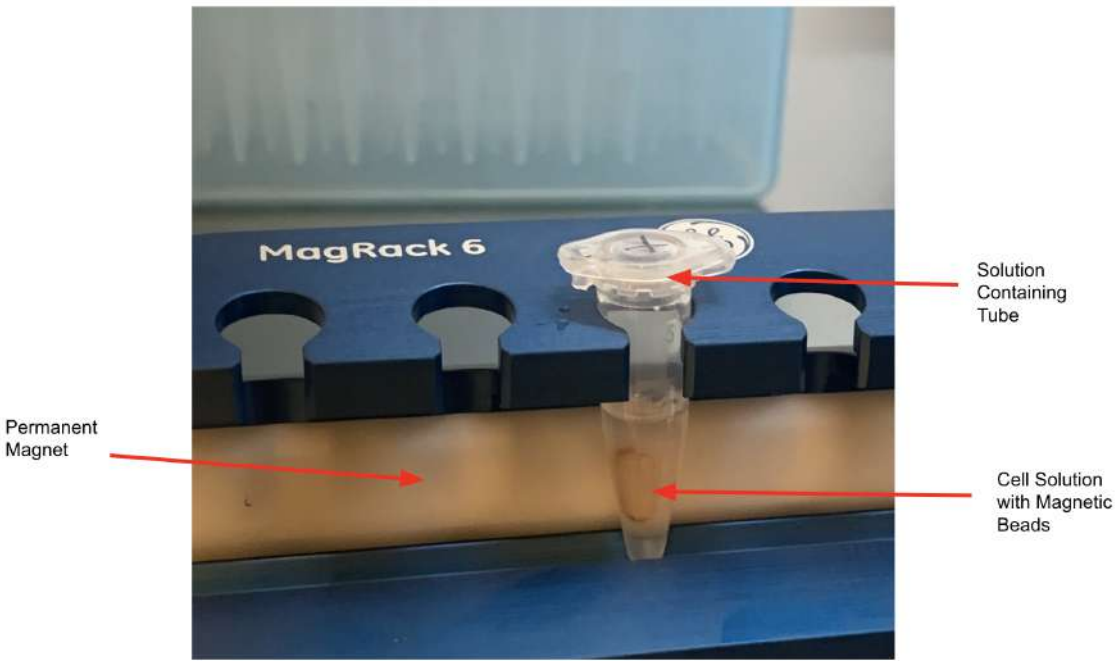

Figure 4.1: Conventional Magnetic Cell Separation Rack

As it can be seen from the Figure 4.1, the holder in the old method only has a permanent magnet inside the white strip on the back. And there is a protruding handle that acts as a small sleeve to hold the tube. Based on this design, it was developed in accordance with the project and the structure shown below was created.

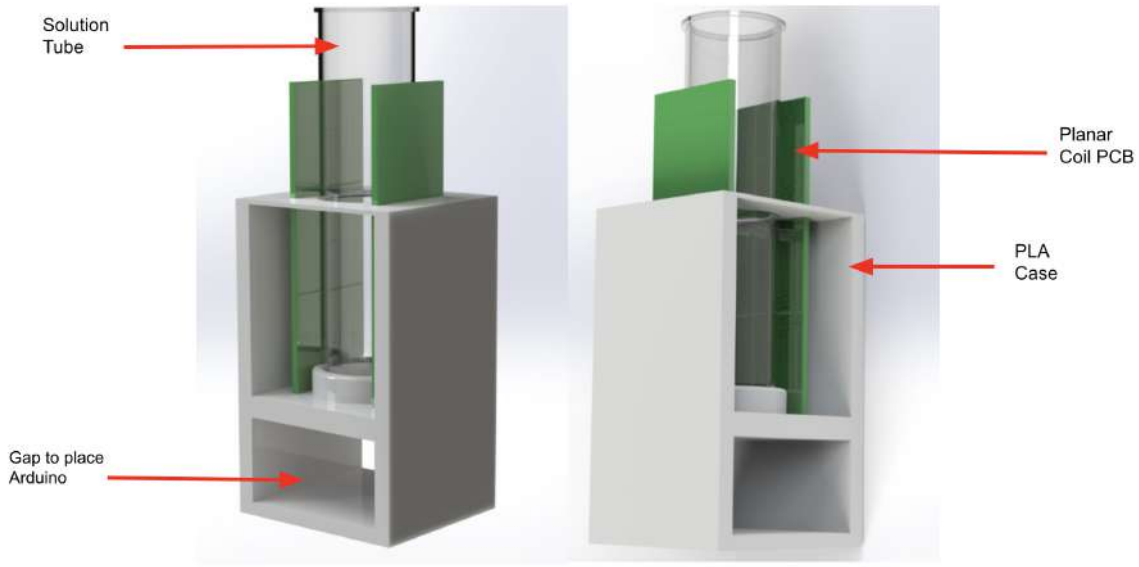

Figure 4.2: 3D Design of the System Holder

The system was constructed to accept three separate tube capacities of: 1.5 mL, 1 mL and 0.5 mL. Their inner diameters and heights are respectively:

- 8.35 mm, 8.27 mm and 8.12 mm
- 28.1 mm, 27.74 mm and 27.23 mm

Three tubes were tested for each planar coil. The magnetic separation rack is intended for small-scale liquid-magnetic bead separations. This handy rack allows you to separate the mixed compounds without having to use your hands. It just takes 15 to 20 minutes for particles to be attracted to the inside surfaces of the tube. The space at the bottom is left to put the arduino uno. For this, the length and width of the Arduino Uno were measured. These dimensions are respectively:

- Length = 68.6 mm
- Width = 53.4 mm

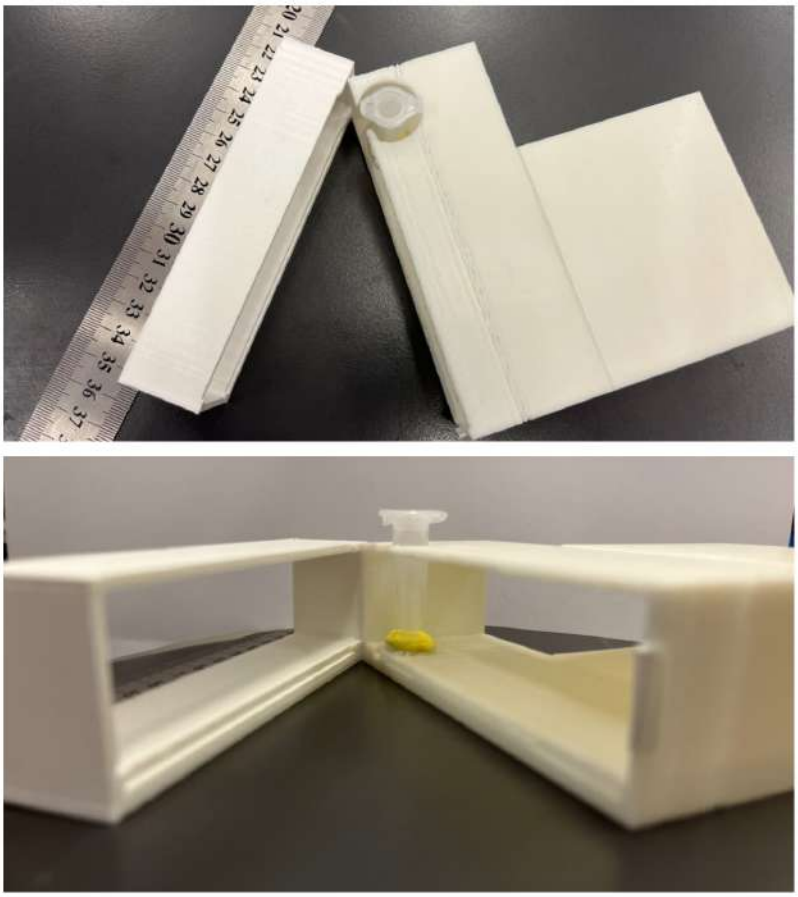

Figure 4.3: Final printed version of 3D tube rack.

As seen in the printed three-dimensional design, there is a space in the dimensions that the tube can fit into, and there are 3 removable parts. One of these parts is made to put the Arduino Uno and the other two are made to fix the planar coil PCBs. It provides convenience when changing PCBs and tubes, as it has two removable and pluggable parts.

5. ELECTRONICS

This chapter presents the electronics part of the system as superficially shown in Chapter 3. Section 4.1 discusses the design of the driver circuit layer according to the limitations.

5.1. Driver Circuit Design

While designing the driver circuit, Arduino Uno was used as microcontroller. The Arduino is fed with an external power source, making the current and voltage changeable, and thus it is aimed to control the current passing through the circuit. This application, which has the same purpose as the use of Darlington Pairs, has been made to optimize the magnetic field that will occur on the planar coils. In this thesis, the specially selected components in the driver circuit are darlington pair transistor and flyback diode, Arduino Uno is preferred as microcontroller.

The purpose of using Darlington pair transistor and flyback diode is to gain current and also to design a circuit that functions as a switch and to provide one-way movement of the current and to save the circuit elements from burning in sudden current increases. The reason for choosing the components is discussed in more detail under this chapter.

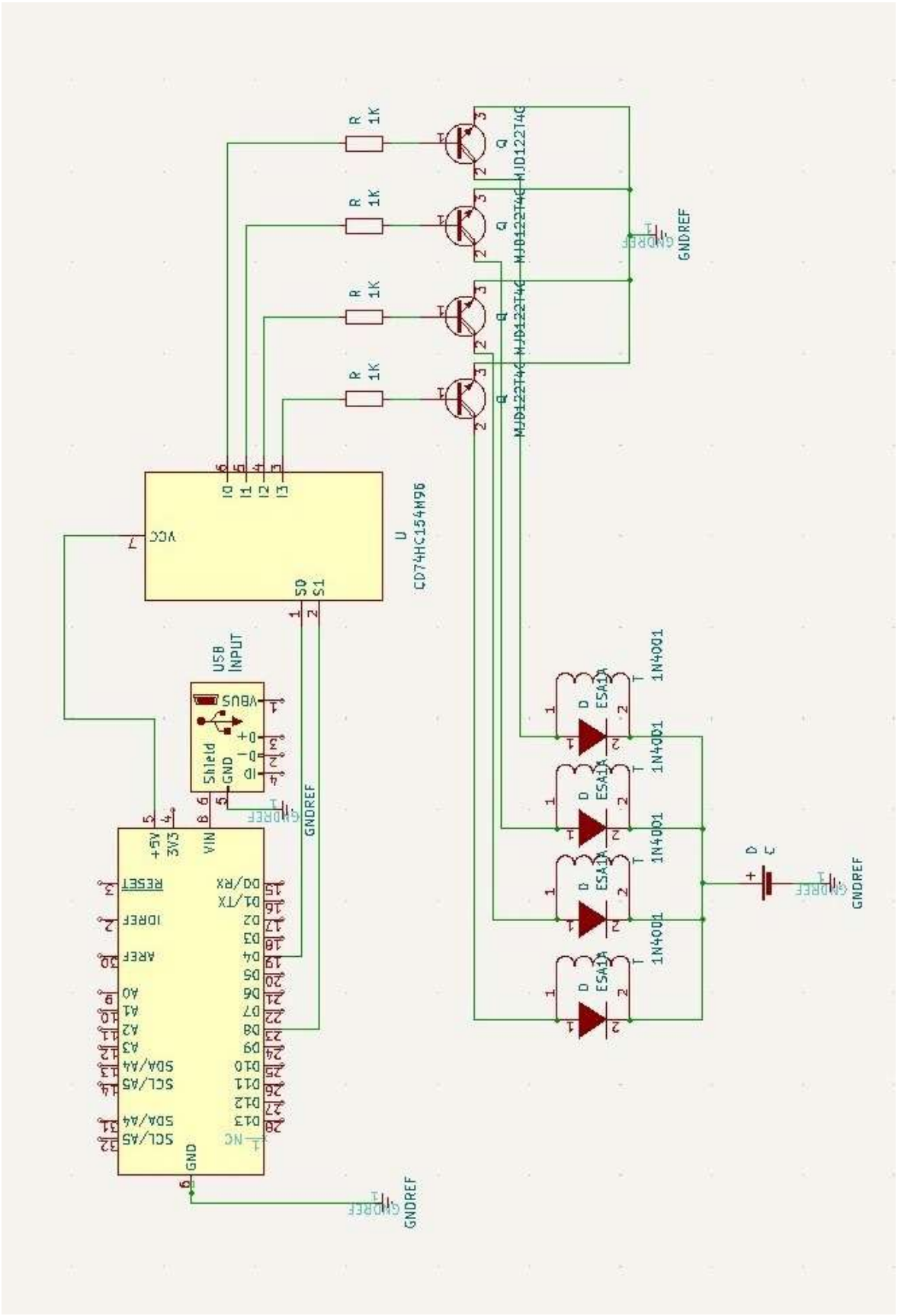

Figure 5.1: Schematic of Driver Circuit

Switches are one of the most common applications for power and Darlington Pair transistors, which are used to turn a DC output "ON" or "OFF" [34]. High-power devices, such as those utilized in this thesis, require more power than a standard logic gate can provide, hence transistor switches are used.

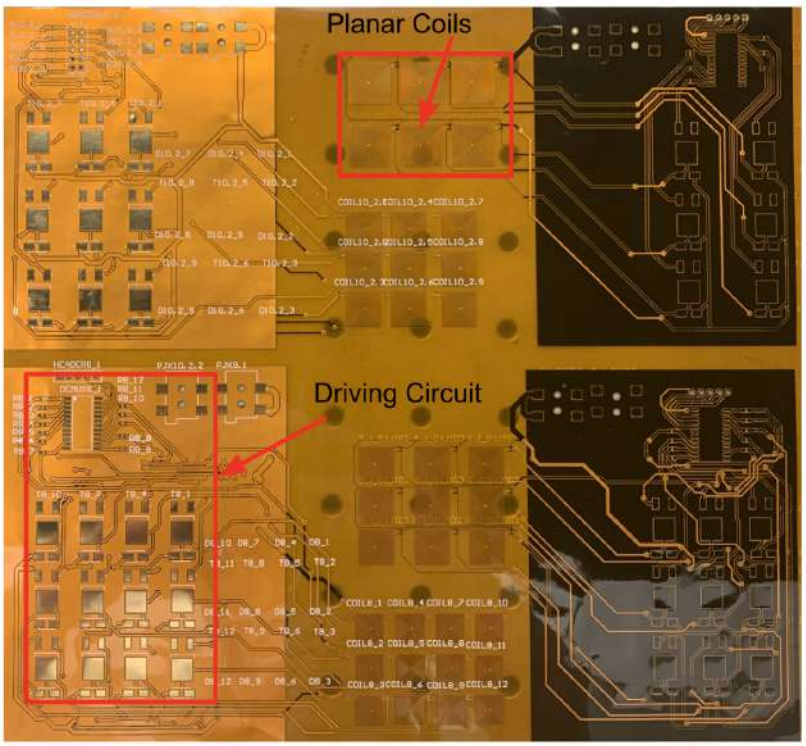

Figure 5.2: Proposed Printed Circuit Board

As can be seen on the printed circuit board, planar coil and driver circuits with different design parameters are printed on PCB. These circuits have been printed and used as a double-sided circuit both in terms of being economical and in order to comply with the area limits. The circuits were ordered and manufactured from PCBWAY.

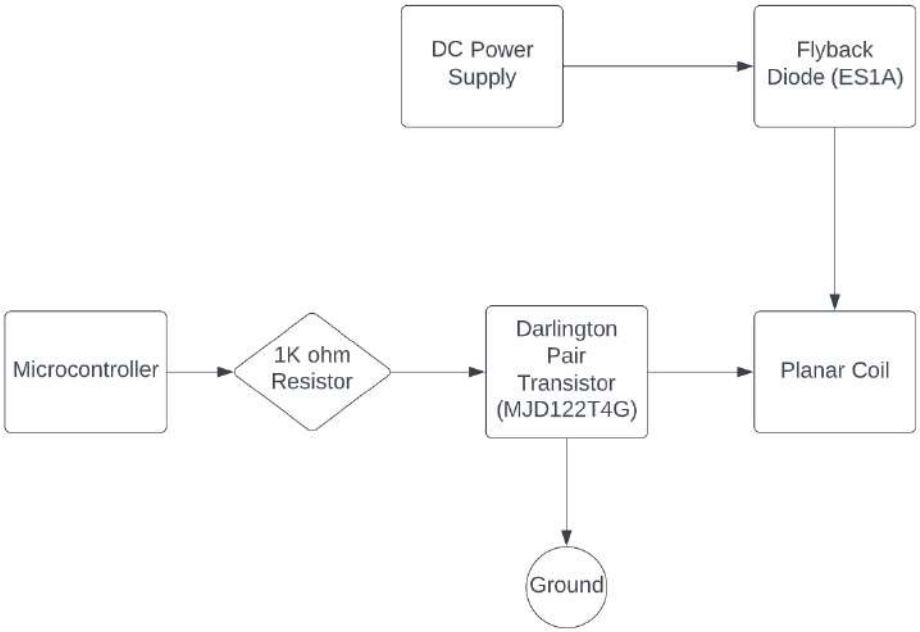

Figure 5.3: Diagram of the Driver Circuit Components

If we consider the working principle of the circuit, Arduino Uno plays a role in switching "ON" and "OFF" the planar coils. Thanks to the code written on Arduino Uno, planar coil arrays are driven as desired. Darlington pair transistor, acts as a switch and helps this ON - OFF operation, and it also provides gain from the magnetic field by increasing the gain from the current. Since the circuit is fed via DC power supply, current and voltage values in various ranges can be given and manipulated.

5.2. Darlington Pair

The Darlington Transistor is a particular arrangement of two ordinary NPN or PNP bipolar junction transistors (BJTs) linked together, named after its creator, Sidney Darlington [1].

The first transistor's emitter terminal is linked to the second transistor's base terminal. As a result, the first transistor receives just the base supply, while the second transistor receives only the output current. As a result, it only has one base, emitter, and collector [35]. Therefore it results with a more sensitive transistor with a significantly higher current gain is produced, which is beneficial in applications requiring current amplification or switching [36].

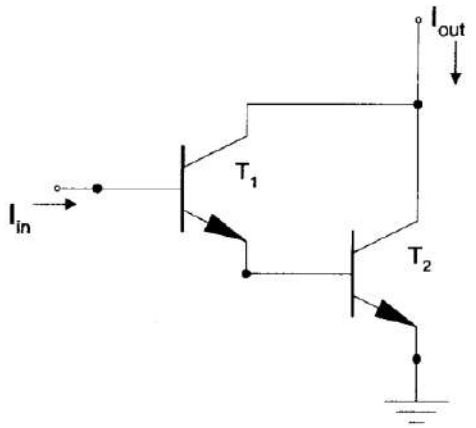

Figure 5.4: Darlington transistor pair. [1]

Darlington Transistor pairs can be made from two individually connected bipolar transistors or from a single device commercially packaged in a single package with the standard: Base, Emitter, and Collector connecting leads, and are available in a wide range of case styles and voltage (and current) ratings in both NPN and PNP versions [37].

Figure 5.2. shows a schematic diagram with transistors T1 and T2 connected as a Darlington transistor pair. The first transistor, often known as the "input," receives the input signal and sends it to its Base. This transistor amplifies it as usual and utilizes it to power the larger "output" transistors. The signal is amplified again by the second transistor, resulting in an extremely high current gain [38]. Darlington Transistors have large current gains when compared to single bipolar transistors, which is one of its key properties [39].

If we ignore the current flowing through the resistors and define the common-emitter current gain for a single transistor as:

$$\beta = I_c/I_b \tag{5.1}$$

the overall dc or low frequency current gain for the darlington pair is:

$$\beta_1 + \beta_2 + \beta_1\beta_2 = I_{out}/I_{in} \tag{5.2}$$

When compared to a regular transistor, a Darlington transistor (or Darlington pair) offers various benefits. They've been summed up in the following list [27, 40]:
- A Darlington transistor's major benefit is its high current gain. Therefore, a little base current is sufficient to activate the transistor.
- It has a high input impedance, which means that the output impedance is reduced as well.
- It is simple to use it on a circuit board or PCB.

Disadvantages have been summed up in the following list [27, 40]:

- Switching velocity is slow.
- Bandwidth of Darlington Pairs are limited.
- Produces a phase difference that, in a circuit utilizing negative feedback, may cause issues at particular frequencies.
- Higher average base-emitter voltage.
- Large saturation voltage (generally 0.7 V).

The purpose of using darlington pair transistors in this thesis is to increase the current. Gaining current from the current is very important to this project because as the current increases, the magnetic field created by the planar coils will increase, thus increasing the attraction force applied to the magnetic beads. Sufficient magnetic field has been obtained even from small coils. Darlington Pair is also employed as a switch in this thesis to turn on and off a load with a microcontroller.

5.3. Flyback Diode

A diode linked across an inductor is understood as a flyback diode. it's accustomed eliminate flyback by having the facility supply's polarity reversed [41]. It's employed in switching power supplies and inverters, moreover as circuits with inductive loads controlled by switches [42].

A flyback diode is placed in parallel across the inductor to avoid the reverse polarity voltage pulse on switch turnoff [42]. The flyback diode's role is to enable an electrical current to flow in one direction alone while blocking it within the other [43]. When the power supply is connected to the relay, the voltage of the inductance coil rises to match the power source's. The time it takes to reduce current flow through the coil in this situation is longer than the time it takes to remove the power supply [43].

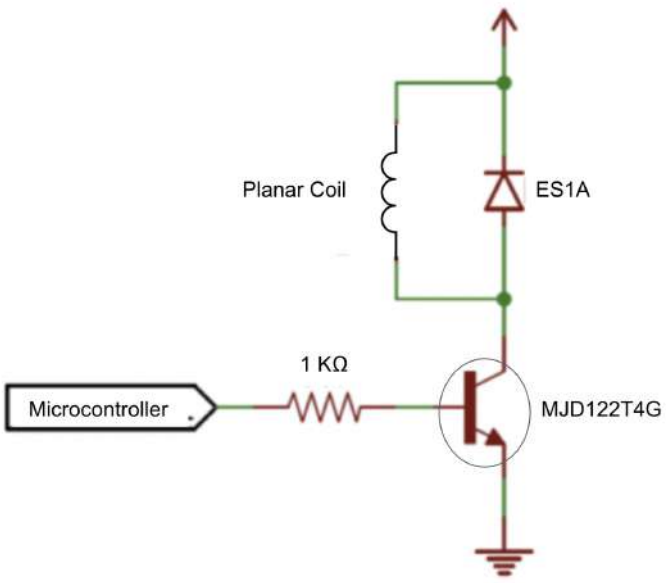

Figure 5.5: Schematic of a flyback diode placed across the inductive load.

A significant voltage potential builds up on the open connections of the component that controls the relay as a result of this. Flyback voltage is the term for the voltage that has built up. It may cause an electrical arc, causing damage to the relay's control components [44].

In this project flyback diode is used to prevent this damage. The transistors that drive the relay coils will be destroyed by the voltage surge, as will the electrical components. When the flyback diodes are linked in reverse bias to the supply voltage, the voltage spike will be in the other direction. Short circuit occurs through the diode when this happens. As a result, the voltage spike across the coil is short-circuited. This will safeguard the circuits that are linked.

6. IMPLEMENTATION

This chapter describes the implementation of the planar coil circuit designed in Chapter 4 and 5. Section 5.1 presents which materials are supplied into the fabrication. Section 5.2 elaborates the fabrication techniques to be able to attain robust. Section 5.3 shows the proposed fabrication process and eventual form of the fabricated.

6.1. Planar Coil Implementation

Three coils with turn numbers of 35, 29 and 23 were explored (since these are the coils that receive the most magnetic field) to compare the performance of planar coils constructed, coils intended to produce a magnetic field: which are indicated in the design specifications correspondingly. The number and placement of target points, as well as the current flow through coils and power dissipation, were all kept constant in each scenario (See table 6.1, 6.2, 6.3). These values are kept constant because when the current is higher than 3.5 Amperes the circuit burns out. Texas Instruments' Coil Designer - WEBENCH® Power Designer was used to create the coils. The elemental Biot-Savart law was used to compute the magnetic field produced by these coils. Gaussmeter was fixed on the coils with a tape before testing and magnetic field values were taken in these measurements.

Voltage (V)	**Current (mA)**	**Magnetic Field (T)**	**Power (mW)**
1.5	260	34 x 10^{-3}	390
2	415	46 x 10^{-3}	830
2.5	586	62 x 10^{-3}	1465
3	785	88 x 10^{-3}	2355
3.5	970	102 x 10^{-3}	3395
4	1222	128 x 10^{-3}	4888
4.5	1374	141 x 10^{-3}	6183
5	1641	163 x 10^{-3}	8205
5.5	1771	181 x 10^{-3}	9740
6	1905	188 x 10^{-3}	11430
6.5	2053	209 x 10^{-3}	13345
7	2184	227 x 10^{-3}	15288

Table 6.1: Tested values of a 23 turned planar coil.

Voltage (V)	**Current (mA)**	**Magnetic Field (T)**	**Power (mW)**
1.5	164	40 x 10^{-3}	246
2	302	65 x 10^{-3}	604
2.5	433	85 x 10^{-3}	1082
3	627	119 x 10^{-3}	1881
3.5	772	154 x 10^{-3}	2702
4	897	172 x 10^{-3}	3588
4.5	1045	227 x 10^{-3}	4702
5	1172	249 x 10^{-3}	5860
5.5	1370	254 x 10^{-3}	7535
6	1506	272 x 10^{-3}	9036
6.5	1565	289 x 10^{-3}	10172
7	1644	301 x 10^{-3}	11508

Table 6.2: Tested values of a 29 turned planar coil.

Voltage (V)	Current (mA)	Magnetic Field (T)	Power (mW)
1.5	193	42 x 10^{-3}	289,5
2	245	96 x 10^{-3}	490
2.5	445	131 x 10^{-3}	1112,5
3	556	163 x 10^{-3}	1668
3.5	703	228 x 10^{-3}	2460,5
4	832	268 x 10^{-3}	3328
4.5	937	306 x 10^{-3}	4216,5
5	1042	335 x 10^{-3}	5210
5.5	1094	357 x 10^{-3}	6017
6	1188	373 x 10^{-3}	7128
6.5	1224	396 x 10^{-3}	7956
7	1280	442 x 10^{-3}	8960

Table 6.3: Tested values of a 35 turned planar coil.

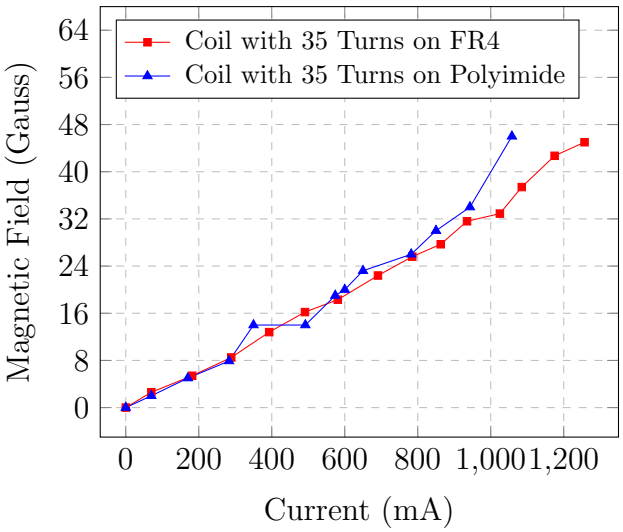

Figure 6.1: Current vs. Magnetic Field Magnitude plots for 35 turn numbered planar coil on polyimide and FR4 substrates.

Magnetic field and current graph can be seen in this graph are observed by driving only a single coil. These test are made to compare the Polyimide and FR4 substrates. As can be seen, the magnetic field values obtained from polyimide and the magnetic field values obtained from FR4 are very close to each other. However, the polyimide material is slightly more effective than FR4. The reason for the deviations in the graph is due to the fact that the circuits get very hot as the repeated tests are made, and different values are taken.

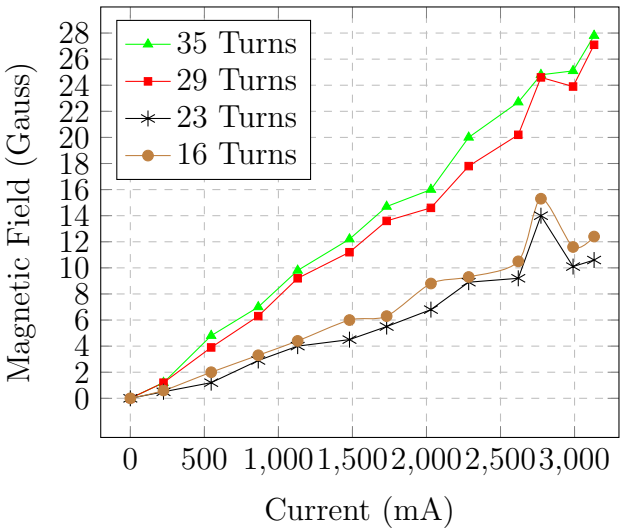

Figure 6.2: Current vs. Magnetic Field Magnitude plots for different sized FR4 printed coils. (Running 4 coil at a time with smd MJD122T4G darlington transistor).

The graph of the tables seen above can be seen in Figure 6.2. The values are taken from this graph are actually very close to what is expected, as the number of turns and the internal diameter increase, the magnetic field from the coils also increases. Since complete combustion is observed after 3 amps in coils with 23 and 16 turns, a higher Tesla value than normally taken before combustion was measured and then this decrease was observed. The instantaneous peak seen in the graph represents the value taken before it burns out.

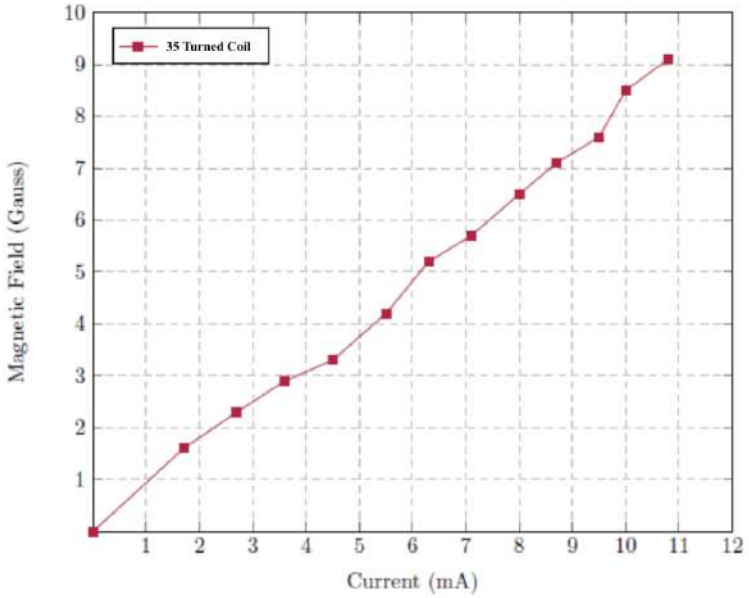

Figure 6.3: Magnetic Field vs. Current plots for 35 turned planar coil on polyimide.

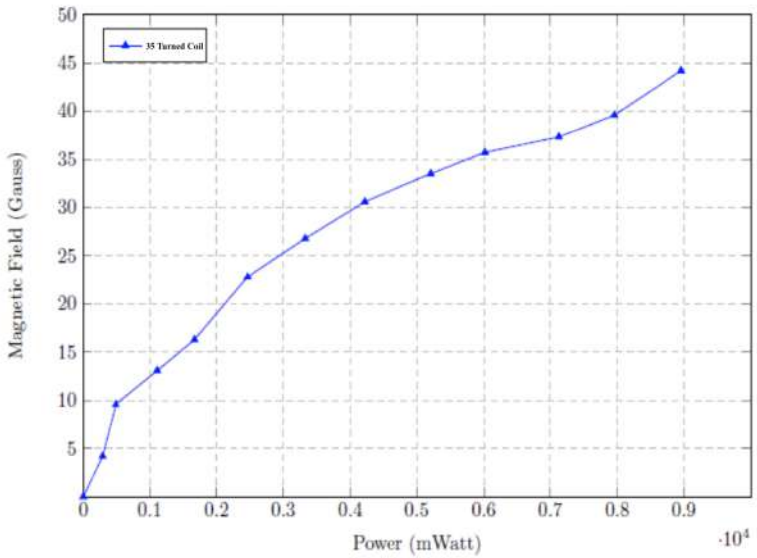

Figure 6.4: Magnetic Field vs. Power plots for 35 turned planar coil on FR4.

These two graphs are based on the best performance planar coil. Since the number of internal turns is the highest, 35 acres planar coil is the planar coil with the highest Tesla in terms of magnetic field. In these two graphs, we see current - magnetic field and magnetic field - power plots. As expected, both graphs increase proportionally.

6.2. Magnetic Beads with Antibodies

Magnetic beads (also referred to as magnetic particles) are one amongst the foremost flexible techniques in biology for separating biomolecules quickly and effectively. Magnetic beads are made of 20 - 30 nm iron oxide particles, such as magnetite (Fe3O4), that give them superparamagnetic characteristics.

Magnetic beads, unlike more typical ferromagnets, only show magnetic activity when exposed to an external field. This paramagnetic feature, which relies on the small size of the particles in the beads, allows the beads to be separated in suspension from whatever they're attached to. They don't attract one another outside of a field of force.

Magnetic cell separation necessitates the employment of magnetic beads that are coated with antibodies that detect certain cell receptors. Because these receptors are specific to the target cell type, they were chosen. When the body's system identifies dangerous molecules called antigens, it produces an antibody. Microorganisms (bacteria, fungi, parasites, and viruses) and chemicals are samples of antigens.

Antibodies are created when the system incorrectly interprets healthy tissue as a threat. This can be categorized as a disease. Antibodies are one-of- a-kind proteins that protect body from a specific variety of antigen. Adoptive T-cell transfer may be a new therapeutic method for cancer that features removing T cells from a patient, expanding and activating them outside of the body, so reinfusing them into the body to focus on tumors.

Beads	M - 280
Diameter (μm)	2.83
CV (%)	1.4
Density (g/cm3)	1.4
Iron (mg/g)	118

Table 6.4: Characterization of Magnetic Beads.

In this thesis, the separation process was observed using magnetic beads attached to cells with colored antibodies. The cells magnetic beads used are Dynabeads™ M-280 Streptavidin by Invitrogen.

Purification of proteins and nucleic acids, protein interaction studies, immunoprecipitation, immunoassays, phage display, biopanning, drug screening, and cell isolation are various uses for DynabeadsTM M-280 Streptavidin. Dynabeads™ Streptavidin are 2.8 m diameter superparamagnetic beads with a streptavidin monolayer covalently attached to the surface. This layer prevents streptavidin leakage, and therefore the absence of excess adsorbed streptavidin provides batch uniformity and repeatability.

T cells, antibodies and other biotinylated molecules are added to a sample containing the beads. Superparamagnetic, monosized polymer beads covered with a thin, inert polymer shell to encapsulate the magnetic substance are InvitrogenTM DynabeadsTM magnetic beads.

Where the standard deviation of the bead diameter, expressed as a percentage of the mean bead diameter, is known as CV.

The beads are transferred to a new tube. Washing procedure of the beads is as follows:

1. Withhold the beads in the tube (by swirling or tilting and rotating).

2. Pour the necessary amount of beads to the tube.

3. Washing buffer is mixed to the magnetic bead solution.

4. Place the tube on the planar coil and dispose the supernatant.

5. Remove the tube from the magnet and withhold the washed beads in the same amount of washing buffer as the beads removed from the tube.

6.3. Design Materials

Lab on chip devices are crucial for flexible applications. As a novelty, this study develops an innovative and cost-effective production approach for various sized planar coil arrays on a polyimide flexible substrate and FR4 rigid substrate.

6.3.1. Properties of FR4

FR4 has good adhesion to copper foil and has minimal water absorption, making it very suitable for normal applications. The term FR4 refers to flame resistance. The fabric is formed of glass-epoxy compounds and may be a composite. [45] FR4 is employed in PCBs that need high mechanical strength. For single-sided, double-sided, and multilayer computer circuit boards, it's the foremost prevalent material. [45]

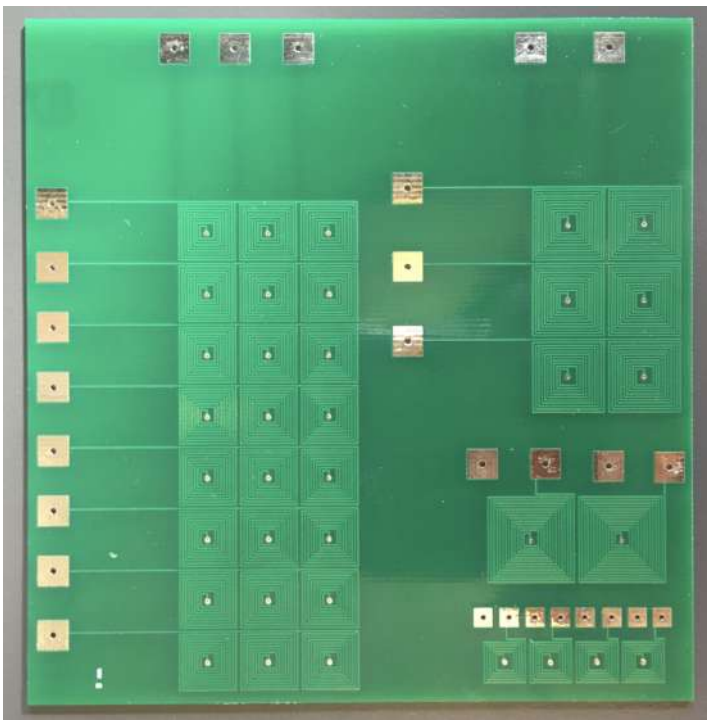

Figure 6.5: Printed planar coil arrays with turn numbers of 35, 29, 23 and 16 on FR4.

The PCB in Figure 6.5 represents planar coils of different sizes printed on FR4. The values in the planar coil tables on FR4, which are also seen in the Implementation Chapter, were tested on this printed circuit board. On the PCB seen, there are coils with 35, 29, 23 and 16 turn numbers and outer diameters of 12 mm, 10 mm, 8 mm and 6 mm, respectively. These planar coils are prepared as a matrix array, so input pads control the intersections of columns with rows.

For most purposes, FR4 is considered the standard PCB material. The following are some of the material's most notable features [46]:

- Excellent Strength-To-Weight Ratio
- Extremely Versatile
- Radiation and Chemically Resistant
- Dimensional Stability
- Great Electrical Insulator

The prepared test board was necessary in this thesis because before the final PCB was created, the optimum values obtained from the planar coils had to be checked and the most effective dimensions had to be selected. As seen in the tables and graphs in Chapter 5, the results obtained are in the expected direction.

6.3.2. Properties of Polyimide

The most prevalent material used in flexible printed circuit boards is polyimide. Imide monomer polyimides are the most commonly used polyimides used in flexible PCBs. [28] The thermal conductivity of this material is much higher than that of FR4. Due to their great heat resistance, mechanical characteristics, and chemical resistance, polyimides are an important family of polymers.

The following are some of the material's most notable features [28]:

- Excellent Tensile Strength
- Over a Wide Temperature Range, Very Stable
- Chemically Resistant to an Exceptional Degree
- Electrical Properties That Are Incredible
- Extremely durable with a wide operating temperature range of -200°C to 300°C
- Outstanding Heat Resistance

Since polyimide material is a very flexible structure, it is a very suitable choice for this thesis. Since its heat resistance is higher than FR4 as seen in the table, it is a sufficient reason to be preferred. And since it is a better conductor, it has been observed that its ability to emit magnetic field is also higher.

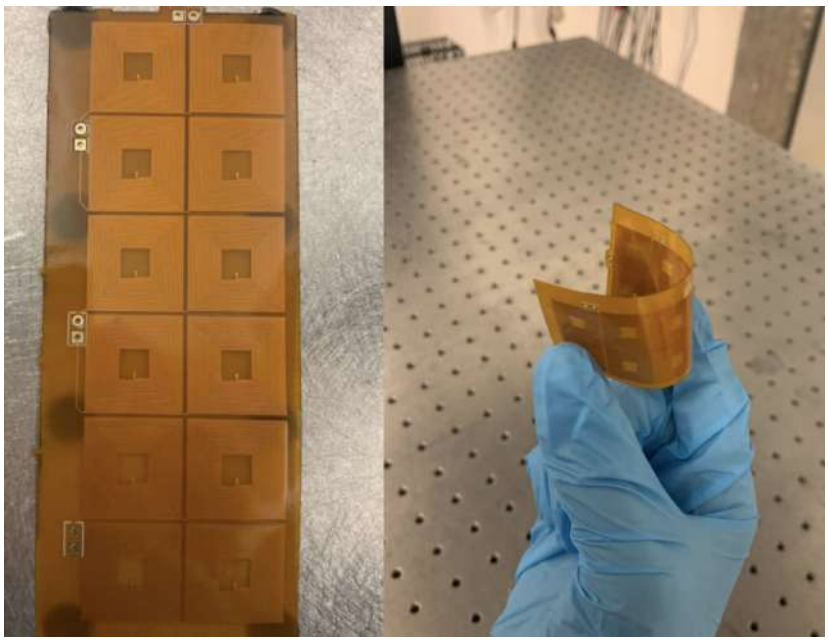

Figure 6.6: Printed planar coil arrays with 35 turns on Polyimide.

The PCB in Figure 6.6 represents planar coils printed on polyimide. The values in the planar coil tables on polyimide, which are also seen in the Implementation Chapter, were tested on this printed circuit board. On the PCB seen, there are coils with 35 turn numbers and outer diameters of 12 mm. These planar coils are prepared as a matrix array, so input pads control the intersections of columns with rows.

As can be seen, polyimide has a bendable and flexible structure. Thanks to these features, a structure that can be wrapped around the tube has been created and used. With polyimide printing, the circuits are made with a planar coil with only 35 turns. The aim here is to compare the strengths and magnetic field differences of the planar coil with the highest magnetic value and the FR4 and polyimide. As can be seen in Chapter 6, the difference between them is graphically illustrated, and polyimide provides slightly better magnetic field and strength than FR4.

Four different PCB printed circuit boards were designed and printed. Planar coil arrays were printed using FR4 and Polyimide materials in order to test the coils only in the first experiments, and the another circuit was prepared using pertinax board and driven from outside. In the final two versions, different models of planar coils in various sizes were printed by adding the driver circuit to the printed circuits.

This thesis uses both materials and test them under the same conditions, which are stated in Chapter 6, to also compare the performance of planar coils with two different materials. Flexible substrates are more resilient, lighter in weight, less expensive, and give superior flexibility to absorb stress. Conformal MEMS devices constructed of flexible substrates are foldable and twistable, making them suitable for mechanically demanding applications. Polyimide was chosen for the flexible substrate in our study because to its superior electrical and thermal insulation, mechanical strength, chemical resistance, and high temperature stability.

7. EXPERIMENTAL WORK

This chapter elaborates on the experimental work of the fabricated planar coil PCBs. Section 7.1 shows the experimental test setups for various qualifications. Section 7.2 explains how the power supply and coils are calibrated to use. Section 7.3 presents the various test results of the experiments.

7.1. Test Setup

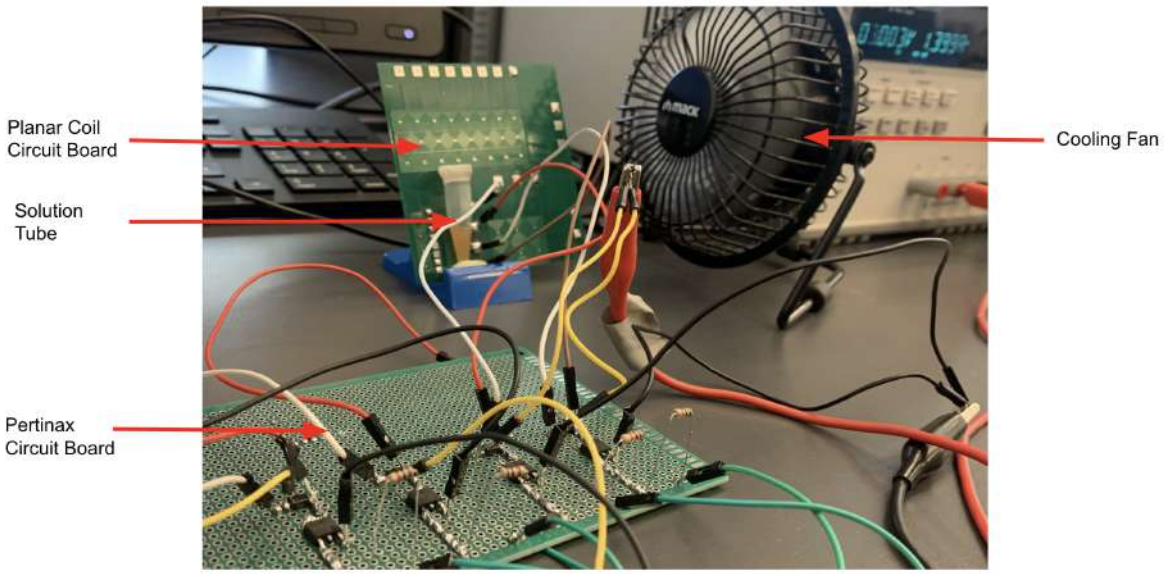

Figure 7.1: Test setup with planar coil arrays using FR4 printed circuit board connected to pertinax circuit board using magnetic bead solution.

In the following step, the proposed planar coil printed circuit boards are tested along with its electronic driver circuit. Generic experimental test setup that composed of (1) a 3D stage to anchor the tube and printed circuit board to the table, (2) a 3-channel power supply (Rohde&Schwarz® HMP3030) to activate the read-out system, (3) a 1-channel power supply (Keysight® E23620A) to start creating a magnetic field from the planar coil, (4) a gaussmeter (AlphaLab® GM2) to measure the magnitude of generated magnetic field, (5) a versatile multimeter (Agilent® 34450A) to measure the changes on the circuit, (6) a PC to connect Arduino Uno are shown in Figure 7.1.

However, the test setups are separated into three different configurations due to various outputs within this experimental work. Since our cell separation process takes a long time (10 minutes for 35 turns, 15 minutes for 29 turns and 20 minutes for 23 turns), we found that the circuit gets very hot when we give 2.5 Amperes and above for more than 5 minutes and the circuit burns out immediately when 3 Amperes flows the circuit board. For this reason, current and voltage values are kept constant at 2 Amperes.

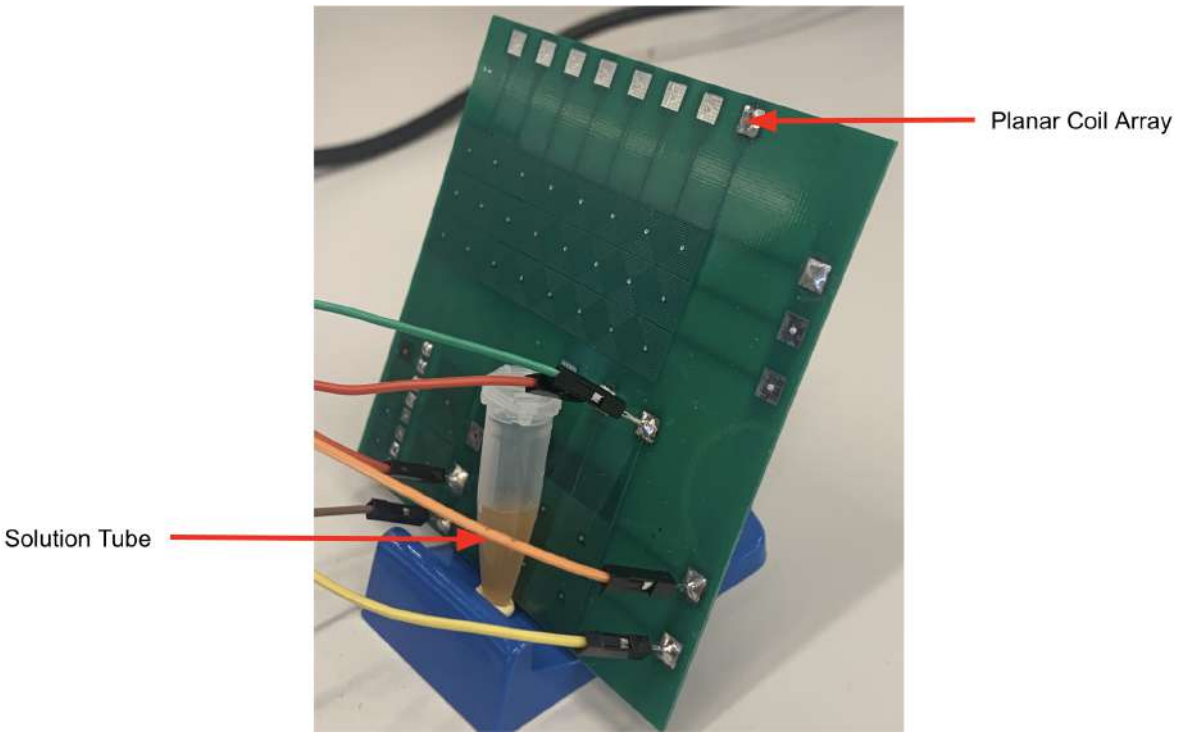

Figure 7.2: Test setup with planar coil arrays using FR4 printed circuit with magnetic bead solution.

As seen in Figure 7.2, the rigid board is attached to the back of the tube. Planar coils touch the tube directly in the setup, which is set to have zero space in between.

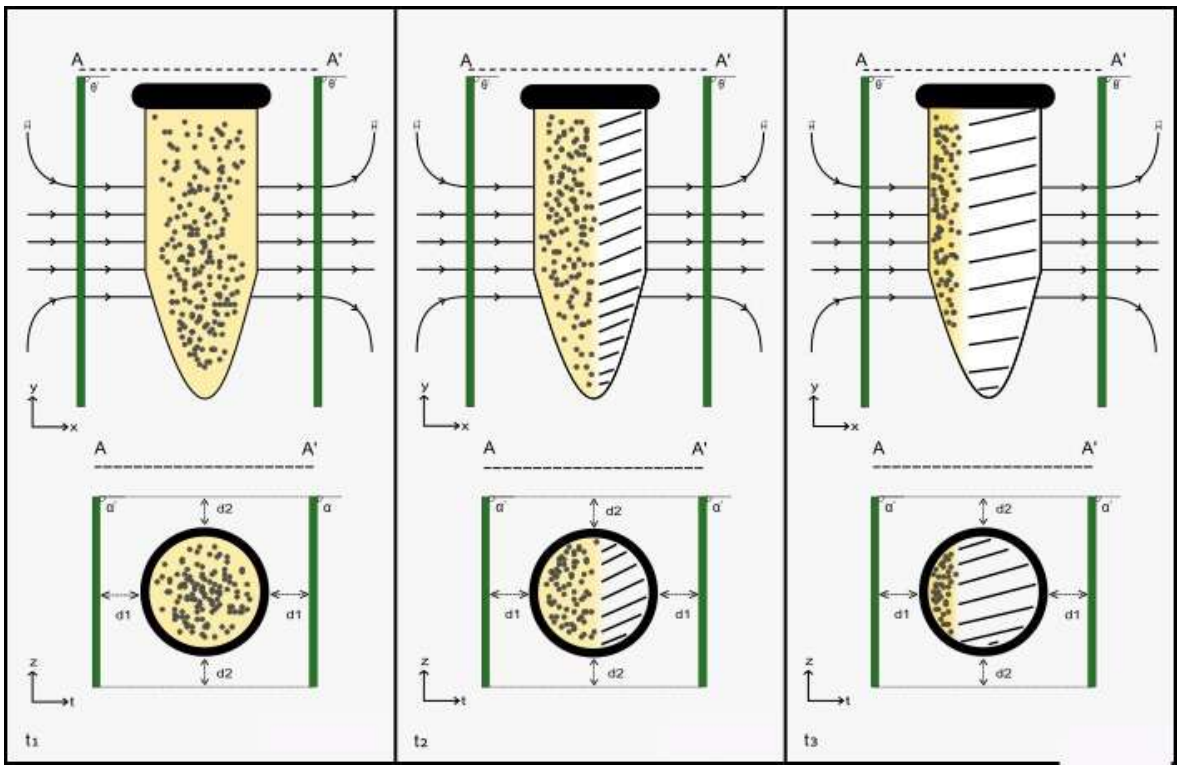

Figure 7.3: Cell isolation system showing the change over time of the magnetic beads affected by the magnetic flux of planar coils.

In the diagram seen in Figure 7.3, magnetic beads are expected to form over time. The magnetic beads, which are initially observed scattered throughout the solution, are expected to be drawn towards the part of the tube that touches the planar coils in the process. As observed in the studies, the effect of magnetic attraction force increases proportionally when the smaller tube is used. A magnetic bead suspension was prepared inside the tube while a current was delivered via the inductors to perform a separation test. The results will be explained in more detail in this chapter.

Results from coils that are first tested with magnetic beads not attached to cells were analyzed using ImageJ. ImageJ is a widely used image analysis application in the biological sciences and beyond. A "binary" (black and white) picture is required for particle analysis. To distinguish the items of interest from the background, a threshold range is defined. The image's pixels with values below the threshold are transformed to black, while those with values above the threshold are converted to white, or vice versa. The areas of the thresholded images were analyzed using the t1, t2 and t3 times taken from the videos of the experiments. Best results are taken by 35 turned planar coil, below there are three different analysis with three different sized tubes. The time course is divided into three:

- t1 = 0, t2 = 5, t3 = 10 minutes for a 35-turn planar coil used with 0.5 mL tube.
- t1 = 0, t2 = 7, t3 = 14 minutes for a 35-turn planar coil used with 1.5 mL tube.
- t1 = 0, t2 = 9, t3 = 18 minutes for a 35-turn planar coil used with 2 mL tube.

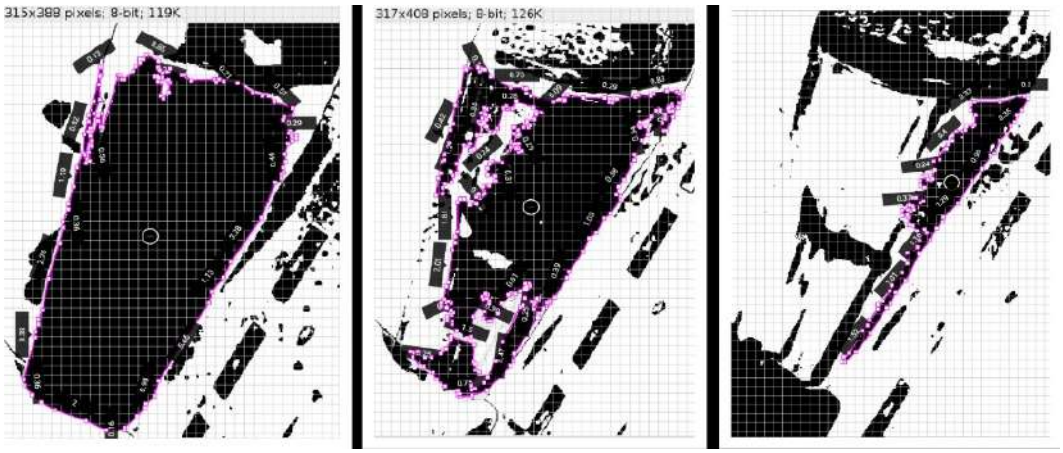

Figure 7.4: Analysis of t1, t2 and t3 using ImageJ with 35 turned planar coil using 0.5 mL tube.

Faster withdrawal is observed when using a 0.5 mL tube. As can be seen in the images passed through the threshold, the magnetic beads were concentrated on the side of the planar coils and the area in the solution gradually decreased as expected.

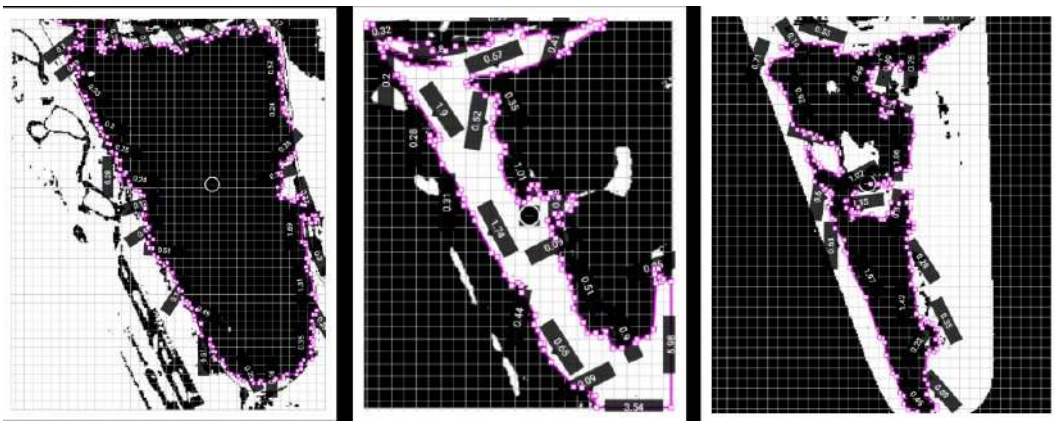

Figure 7.5: Analysis of t1, t2 and t3 using ImageJ with 35 turned planar coil using 1.5 mL tube.

Slower withdrawal is observed when using a 1.5 mL tube when compared to the results taken from 0.5 mL tube. As can be seen in the images passed through the threshold, the magnetic beads were concentrated on the side of the planar coils and the area in the solution gradually decreased but the area of the magnetic beads at time t3 of 1.5 mL tube test is still higher than the area at time t3 of 0.5 mL tube test.

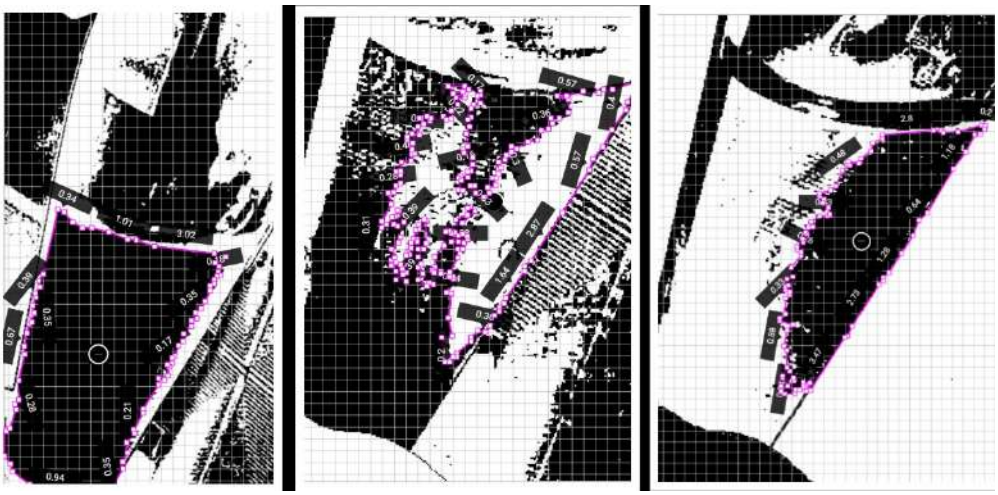

Figure 7.6: Analysis of t1, t2 and t3 using ImageJ with 35 turned planar coil using 2 mL tube.

The slowest withdrawal is observed when using a 2 mL tube when compared to the results taken from 0.5 mL and 1.5 mL tubes. As can be seen in the images, the magnetic beads were concentrated on the side of the planar coils and the area in the solution decreased but the area of the magnetic beads at time t3 of 2 mL tube test is still higher than the area at time t3 of other tubes tests.

A faster shrinkage is observed in the 0.5 mL tube compared to 1.5 mL and 2 mL tubes. Since the diameter of the tube is smaller (See the dimensions of the tubes Figure 4.2: Description and physical dimensions of the microcentrifuge tubes surveyed.), the area where the magnetic beads are located is also reduced, and since the difference between the planar coils and the tube is reduced, the access to those beads is also accelerated.

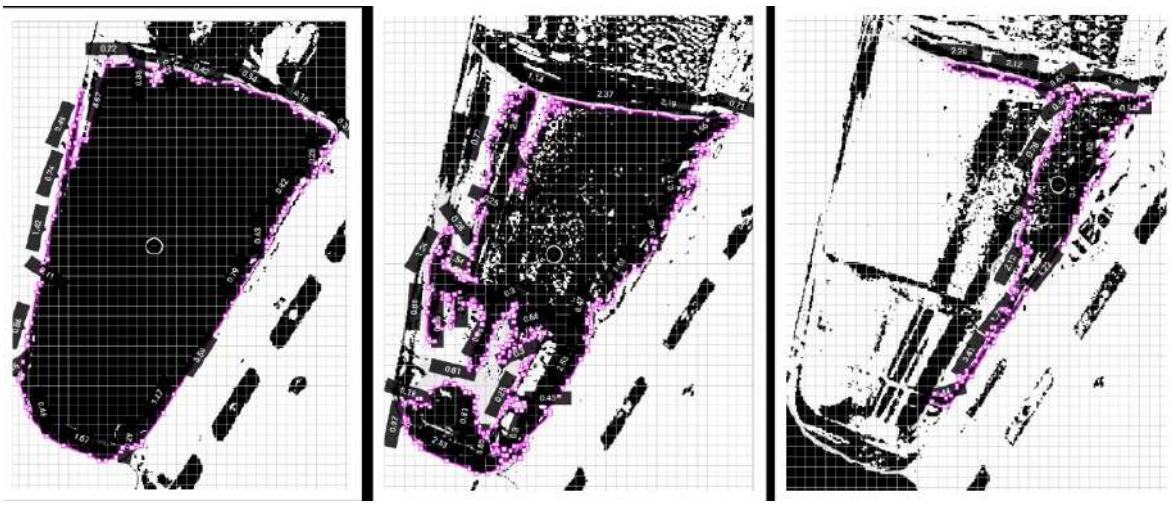

Figure 7.7: Analysis of t1, t2 and t3 using ImageJ with 35 turned planar coil with Polyimide PCB.

The withdrawal is observed when using a 0.5 mL tube that's why when testing with planar coils on polyimide circuit board, 0.5 mL tube is used. As can be seen in the images, the magnetic beads were concentrated on the side of the planar coils and the area in the solution decreased and the area of the magnetic beads at time t3 of the planar coils on polyimide substrate is %0.0234 higher same as the area at time t3 of planar coils on FR4 substrate.

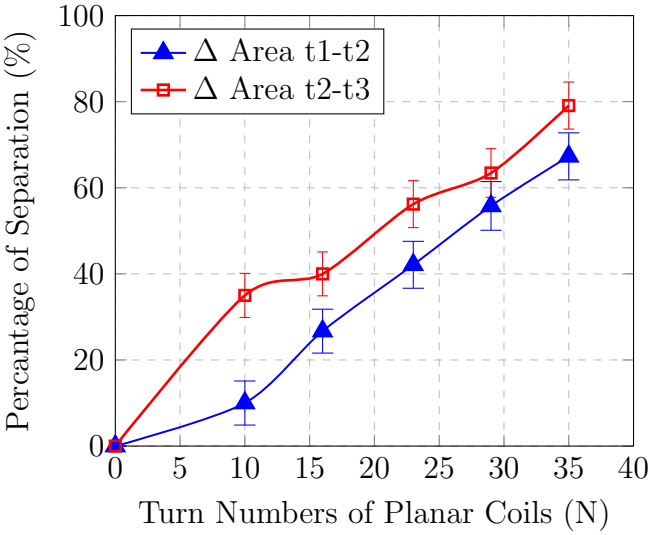

Figure 7.8: An Area Change graph of the ImageJ Analyzed Binary Images that shows the normalized magnetic beads area change depending on the planar coil's turn number using 0.5 mL tube.

Assuming that the solution is uniform and homogeneous (isotropic), the rate of removal of magnetic beads from the solution using the (recommended) system is 84.567 percent (%) when using 0.5 mL tube with 35-turns planar coil on the graph shown in Figure 7.8.

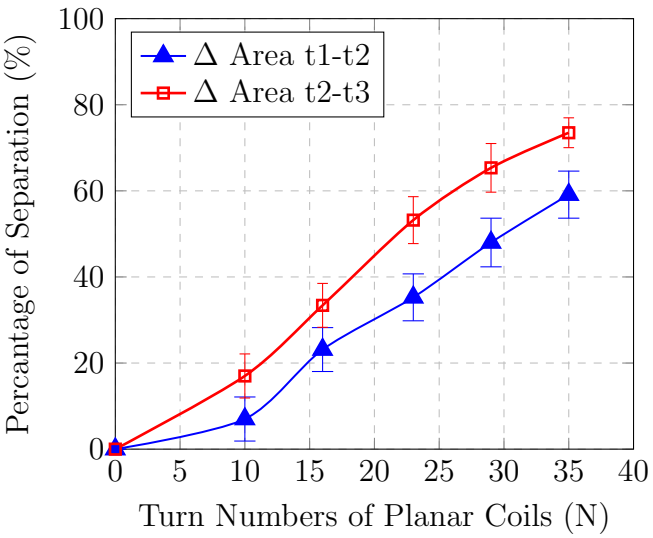

Figure 7.9: An Area Change graph of the ImageJ Analyzed Binary Images that shows the normalized magnetic beads area change depending on the planar coil's turn number using 1.5 mL tube.

Assuming that the solution is uniform and homogeneous (isotropic), the rate of removal of magnetic beads from the solution using the (recommended) system is 76.946 percent (%) when using 1.5 mL tube with 35-turns planar coil on the graph shown in Figure 7.9.

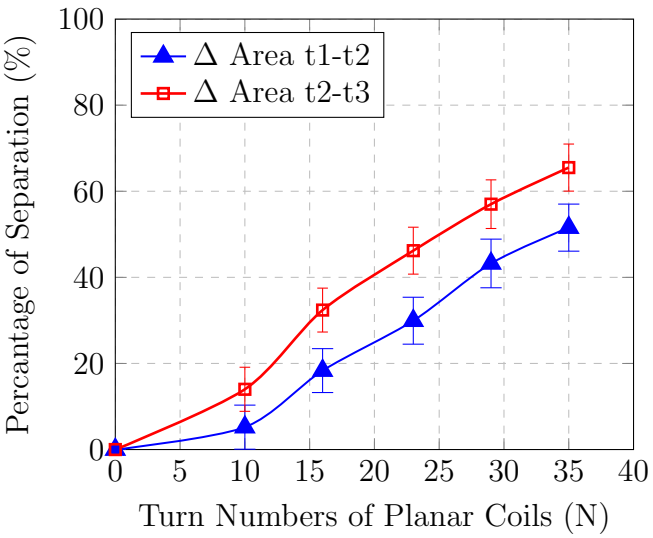

Figure 7.10: An Area Change graph of the ImageJ Analyzed Binary Images that shows the normalized magnetic beads area change depending on the planar coil's turn number using 2 mL sized tube.

Assuming that the solution is uniform and homogeneous (isotropic), the rate of removal of magnetic beads from the solution using the (recommended) system is 71.967 percent (%) when using 2 mL tube with 35-turns planar coil on the graph shown in Figure 7.10.

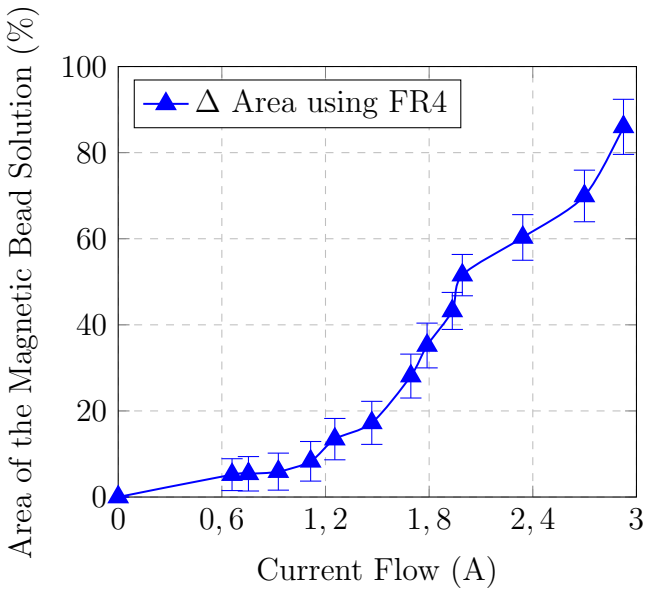

Figure 7.11: An Area Change graph of the ImageJ Analyzed Binary Images that shows the normalized magnetic beads area change depending on the planar coil's turn number using 0.5 mL tube comparing FR4 substrate printed planar coils.

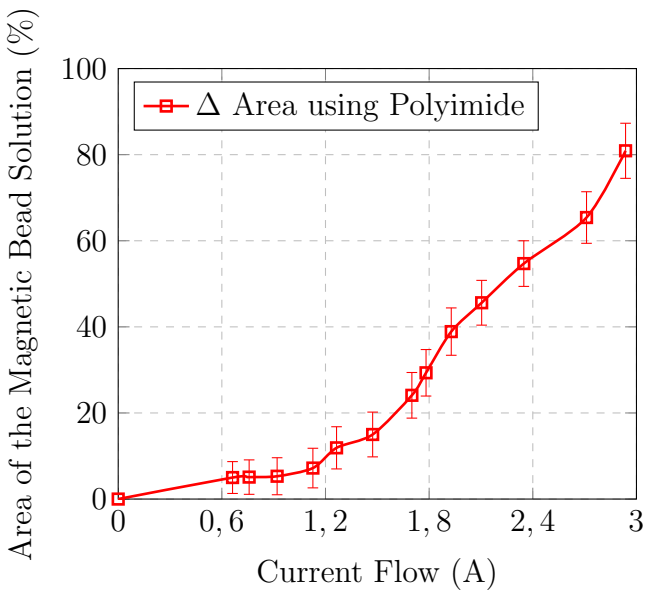

Figure 7.12: An Area Change graph of the ImageJ Analyzed Binary Images that shows the normalized magnetic beads area change depending on the planar coil's turn number using 0.5 mL tube comparing polyimide substrate printed planar coils.

Assuming that the solution is uniform and homogeneous (isotropic), the comparison of the coils on the FR4-printed circuit board, which is 84.567 % free of magnetic beads thanks to the (recommended) system used, and the planar coils printed on the polyimide-printed circuit board is seen. There is only 2.733 percent (%) difference in the use of these two different substrates. The value taken from the circuit printed on the polyimide is 86.7%.

As a second test setup, a solution with magnetic beads connected to live T cells is also tested using known negative and positive magnetic separation techniques. The solution is prepared for the measurement over the PCR Operating Cabinet. Here, the experiment's main objective is to determine the effectiveness using alive cells by our system. By using Eppendorf Pipes magnetic bead solution containing liquid is taken by drawing.

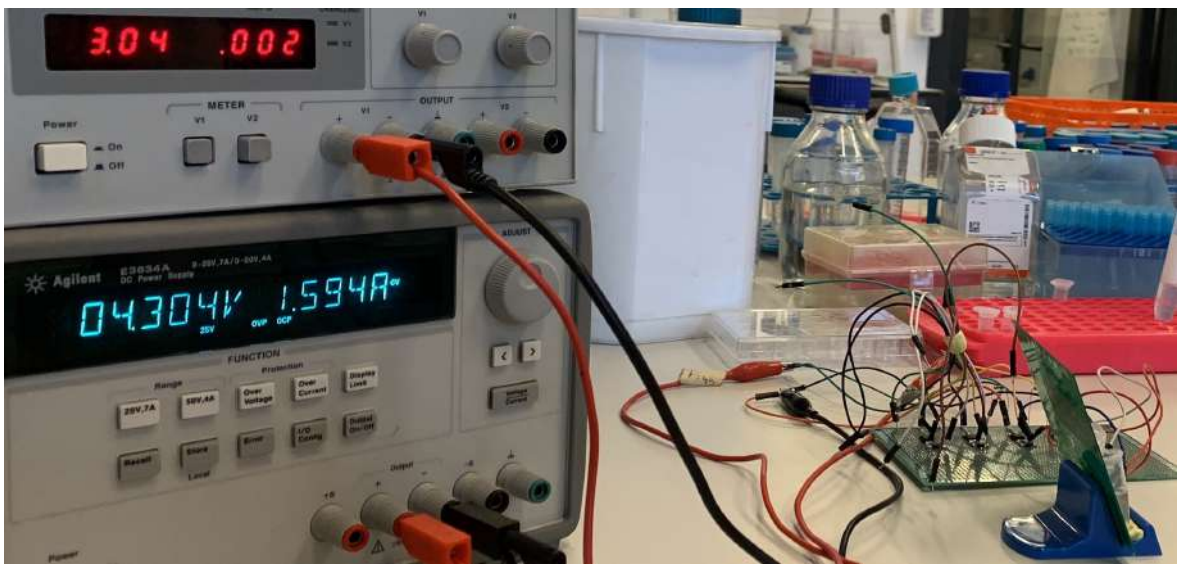

Figure 7.13: Test setup using alive T cells, instead of only using magnetic beads this setup shows the footage of using antibody and magnetic bead binded T cell separation setup.

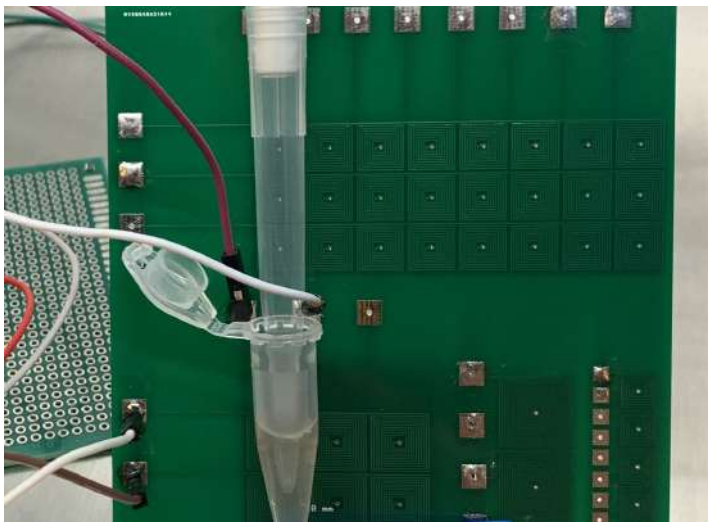

Figure 7.14: Usage of Eppendorf Pipe.

Since the planar coils are still connected to the power supply and working, the magnetic beads sticking to the sides of the tube do not penetrate into the solution drawn with the Eppendorf Pipette. Thus, when examined under the microscope, only cells are observed in the solution taken from negatively selected cells and cells attached to magnetic beads are observed in solution that is positively selected.

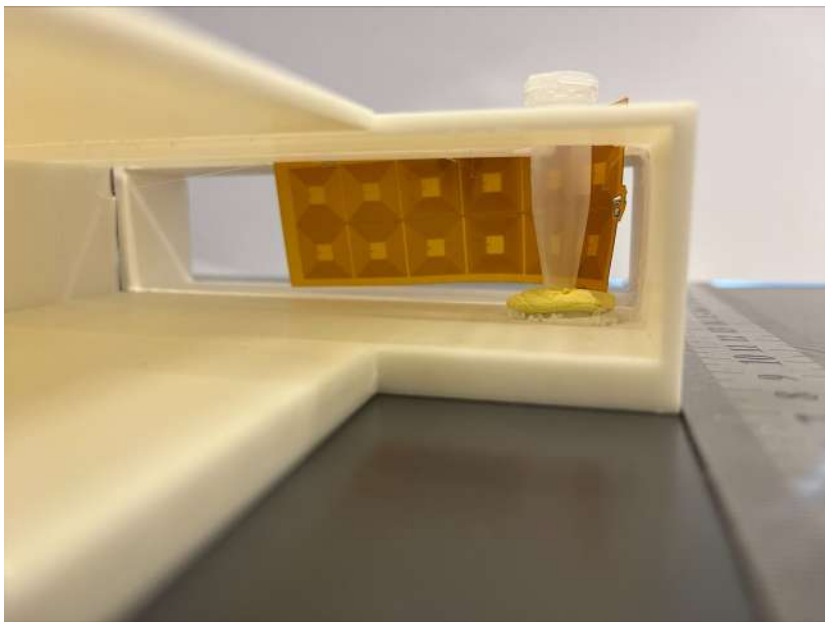

Figure 7.15: Three dimension (3D) Platform Setup for Polyimide Printed Planar Coils.

The last setup configuration is settled in order to measure the polyimide printed planar coil's test results varying from samples in positively and negatively selected cells. The coil is positioned owing to fixing to a three dimension system holder.

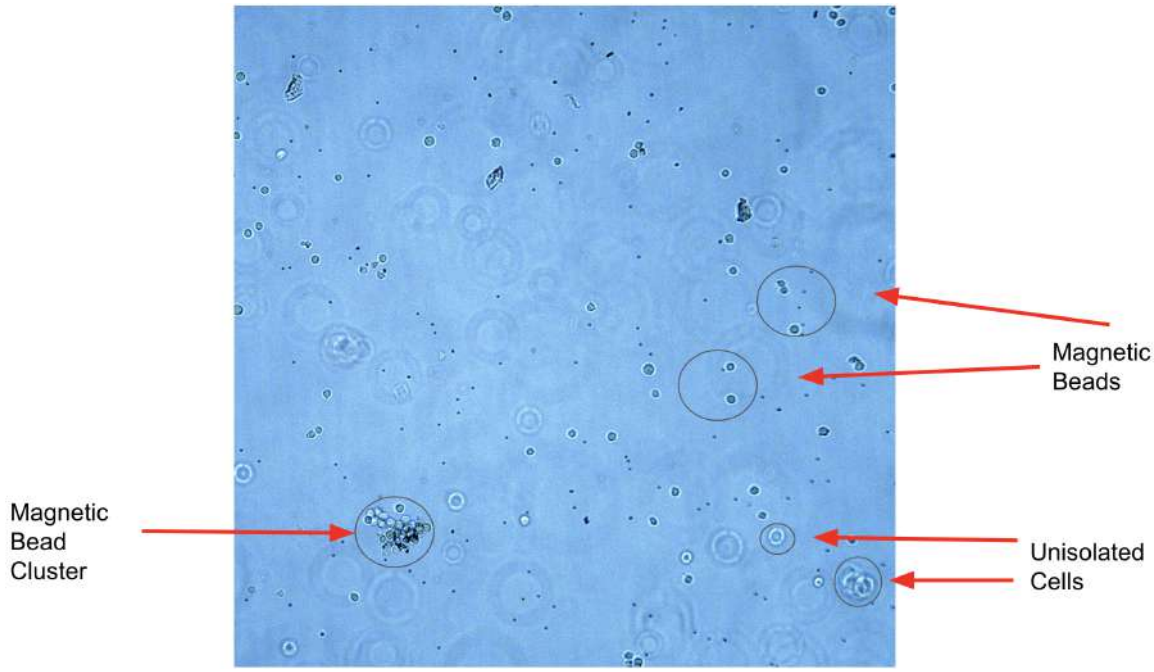

Figure 7.16: Negatively selected solution footage, which includes magnetic beads, under microscope.

If species-specific chemicals are not accessible, the negative separation approach is utilized, but in this thesis negative selection is used to double check the magnetic cell separation system. In the Figure 7.16, the image of the negatively separated solution under the microscope is seen. As it can be seen, there are more magnetic beads than cells in the solution, which is the expected and desired result. Of course, as explained in the previous section, since the system has a margin of error, it has been determined that cells are also present, although they should not be in the separated solution. A cleaner submicron image is expected in a negatively selected solution than a positively selected solution, and this is an expected result.

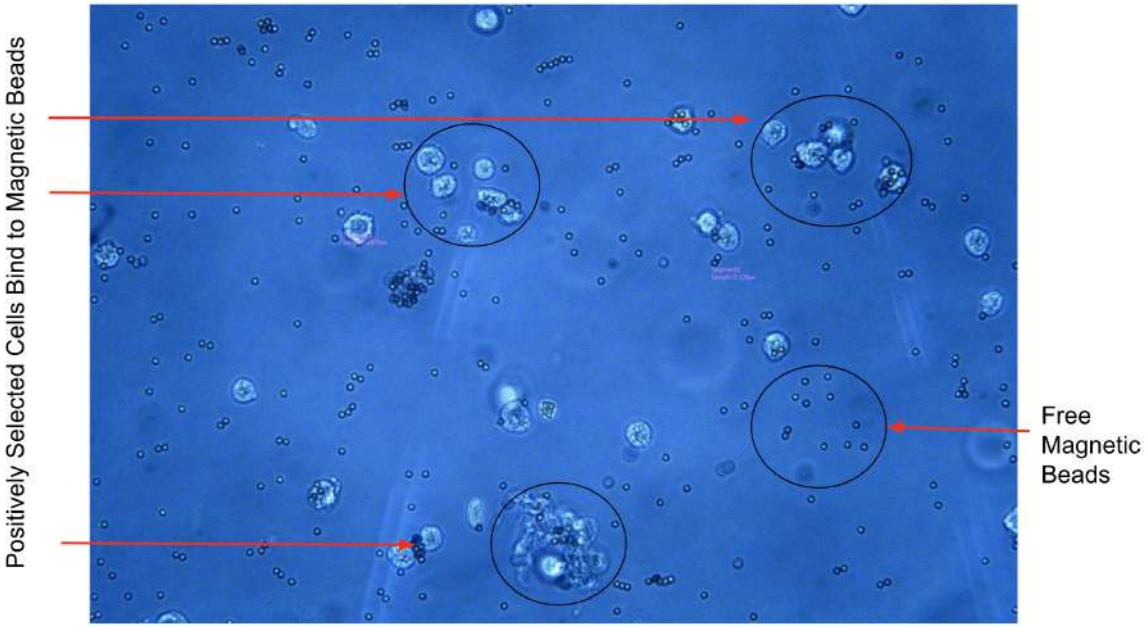

Figure 7.17: Positively selected cell solution footage, which includes magnetic beads connected to alive T cells, under microscope.

Positive selection is the process of isolating a particular cell population using an antibody that binds to that population selectively. In the Figure 7.17, the image of the positively separated solution under the microscope is seen. As it can be seen, there are magnetic beads that are bind to cells and free magnetic beads which are not connected (bind) to any cell in the solution, which is the expected and desired result. Of course, as explained in the previous section, since the system has a margin of error, it has been determined that cells which are not bind to any magnetic bead are also present, although they should not be in the separated solution.

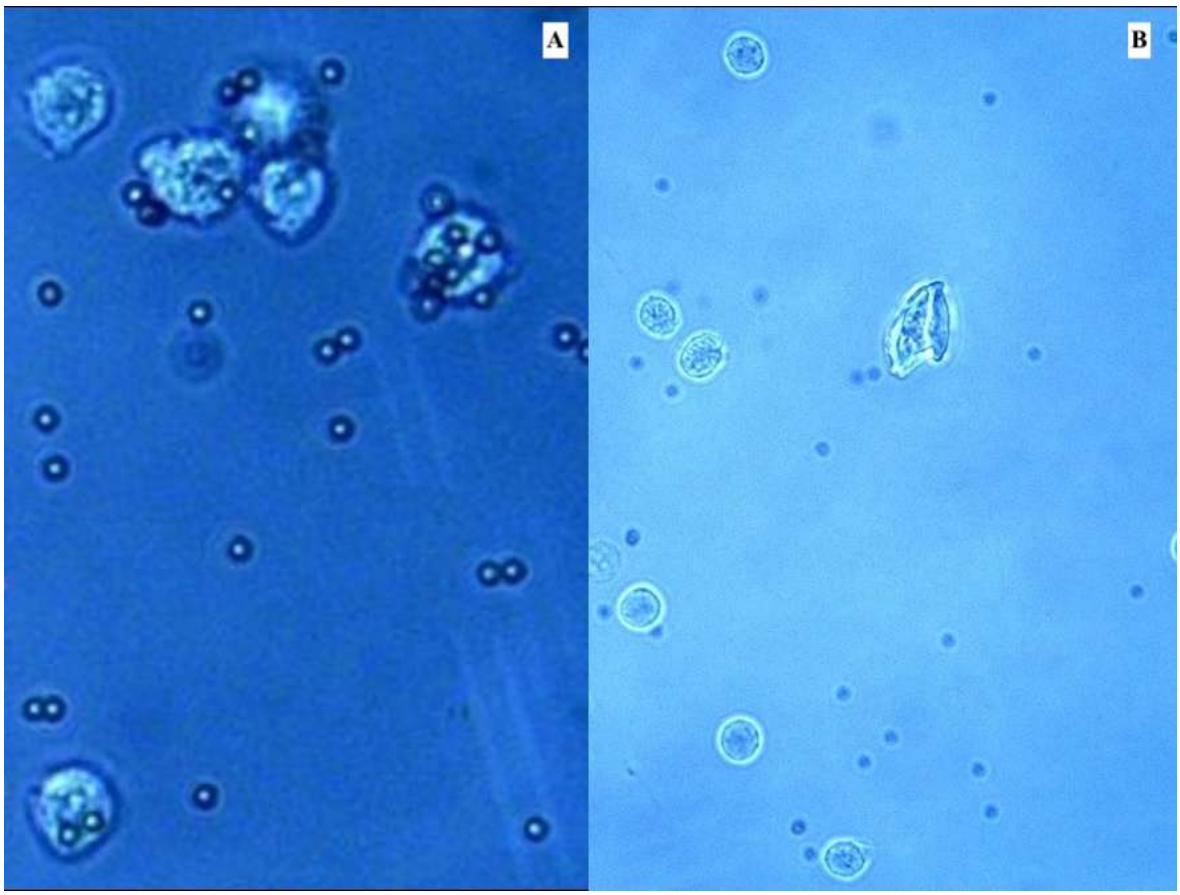

Figure 7.18: The above figure shows T cells positively and negatively attached to magnetic beads. Figure A is a close-up view of cells bound by magnetic beads, while Figure B shows cells that are not bound (free) by magnetic beads.

8. DISCUSSION

This study aims to design and fabricate a new method for magnetic cell separation. Numerous fabrication materials and methods are elaborated with comparing in the literature. In that vein, it has been reported that FR4 and Polyimide structures are both suitable for developing electromagnetic devices in the medical field since they are cheap, off-the-shelf, easy and quick-to-fabricate.

As elucidated above chapters, within this thesis, we proposed FR4 (Rigid) and Polyimide (Flexible) based, easy and quick-to-fabricate, printed circuit board having double layered different sized planar coils to measure the total magnetic field output. In this work, the working principles of a simple magnetic cell separator is improved using this proposed magnetic cell separation methodology. Also, the sensitivity of planar coil printed circuit boards, which are used old-fashioned and unrepeatable fabrication methods is enhanced. Our work does not aim to separate cells high-sensitively, but it proposes a novel method which decreases damage of the cells.

The planar coil size that gets optimum efficiency is selected by checking the planar coil tests performed. However, it was a priority to develop the arduino code used in the tests to create a dynamic array with the selected planar coil and to apply each passive matrix one by one using a passive matrix array.

At the same time, the performance, efficiency and success rates received in projects using polyimide and FR4 are very high and therefore it stands out as an innovative material comparing project that can be used in new design constructions. The biggest problem was that the circuit heats up and sometimes even burns out because too much high current is used. For this reason, an optimum current level was chosen and the experiments were completed in this way by keeping it constant for all and also we used an externally installable cooling fan to solve the problem.

In the future studies of the project, polyimide substrate can be tested by using more, considering the results obtained, there is only 2.733 % difference between polyimide and FR4. And according to these results, polyimide is a slightly stronger substrate than FR4 in spreading magnetic field and thus in magnetic cell separation. It should also be taken into account that in order to develop the wrappable and flexible structure to locate as a sleeve around the tube in the following processes and future work, planar coils can be printed in different sizes and shapes. Only square planar coils were used in the content of this project. In the future, it can be further developed by using round, triangular or specific shapes instead of square planar coils.

9. CONCLUSION

In this thesis, a a new method for magnetic cell separation system with planar coil arrays has been designed, fabricated, and tested as an alternative method for magnetic cell separation. Here it is not aimed to propose a gold standard separation device, but we have presented efficient, point-of-care, harmless to cells and sufficiently sensitive device with a novel method. The demonstrated system is designed to achieve this qualified separation operation with two different materials. For that purpose, the main fabrication materials of the proposed printed circuit board are FR4 and Polyimide.

It was aimed to develop a more sensitive and less harmful structure compared to the old methods. By using square planar coils of different sizes and turns, first the values to optimize the planar coil design were found, and then the magnetic field comparison was made by printing on two different substrates as FR4 and polyimide. According to the results obtained, a 20% less harmful structure has been developed, although it is slower than the traditional method. After the overheating problem of the circuit was resolved, the damage to the cells approached almost zero. Although cell selection does not contain 100% purity, our project has made it a preferable system since it is less harmful to living cells. At the same time, being able to be converted into a flexible structure and being able to manipulate the cells inside from the periphery of the tube is a very innovative approach compared to traditional methods of unilateral cell separation. As can be seen in the Experimental Results Chapter, the results obtained were successful and a successful alternative method to the traditional method could be proposed.

REFERENCES

1. Hodges, D. A., "Darlington's contributions to transistor circuit design", *IEEE Transactions on Circuits and Systems I: Fundamental Theory and Applications*, Vol. 46, No. 1, pp. 102–104, 1999.

2. Sharpe, P. T., *Methods of cell separation*, Elsevier, 1988.

3. Kuhara, M., H. Takeyama, T. Tanaka and T. Matsunaga, "Magnetic cell separation using antibody binding with protein a expressed on bacterial magnetic particles", *Analytical chemistry*, Vol. 76, No. 21, pp. 6207–6213, 2004.

4. Pretlow, T. G. and T. P. Pretlow, *Cell separation: methods and selected applications*, Academic Press, 2014.

5. Ji, H. M., V. Samper, Y. Chen, C. K. Heng, T. M. Lim and L. Yobas, "Silicon-based microfilters for whole blood cell separation", *Biomedical microdevices*, Vol. 10, No. 2, pp. 251–257, 2008.

6. Andersen, M. H., D. Schrama, P. thor Straten and J. C. Becker, "Cytotoxic T cells", *Journal of Investigative Dermatology*, Vol. 126, No. 1, pp. 32–41, 2006.

7. Zhang, Q., T. Yin, R. Xu, W. Gao, H. Zhao, J. G. Shapter, K. Wang, Y. Shen, P. Huang, G. Gao *et al.*, "Large-scale immuno-magnetic cell sorting of T cells based on a self-designed high-throughput system for potential clinical application", *Nanoscale*, Vol. 9, No. 36, pp. 13592–13599, 2017.

8. Miltenyi, S., W. Müller, W. Weichel and A. Radbruch, "High gradient magnetic cell separation with MACS", *Cytometry: The Journal of the International Society for Analytical Cytology*, Vol. 11, No. 2, pp. 231–238, 1990.

9. Lee, W., P. Tseng and D. Di Carlo, *Microtechnology for cell manipulation and*

sorting, Springer, 2017.

10. Yıldırım, I., B. Sarioglu and Y. Gokdel, "3D Printed Head for a Handheld Laser Scanning Confocal Microscope", *Instruments and Experimental Techniques*, Vol. 64, No. 2, pp. 301–307, 2021.

11. Xu, H., Z. P. Aguilar, L. Yang, M. Kuang, H. Duan, Y. Xiong, H. Wei and A. Wang, "Antibody conjugated magnetic iron oxide nanoparticles for cancer cell separation in fresh whole blood", *Biomaterials*, Vol. 32, No. 36, pp. 9758–9765, 2011.

12. Ohara, T., H. Kumakura and H. Wada, "Magnetic separation using superconducting magnets", *Physica C: Superconductivity*, Vol. 357, pp. 1272–1280, 2001.

13. Borlido, L., A. Azevedo, A. Roque and M. Aires-Barros, "Magnetic separations in biotechnology", *Biotechnology advances*, Vol. 31, No. 8, pp. 1374–1385, 2013.

14. Zborowski, M. and J. J. Chalmers, *Magnetic cell separation*, Elsevier, 2011.

15. Kawabe, K., H. Koyama and K. Shirae, "Planar inductor", *IEEE Transactions on Magnetics*, Vol. 20, No. 5, pp. 1804–1806, 1984.

16. Sasada, I. and Y. Nakashima, "Planar coil system consisting of three coil pairs for producing a uniform magnetic field", *Journal of applied physics*, Vol. 99, No. 8, p. 08D904, 2006.

17. Matsuki, H., N. Fujii, K. Shirakawa, J. Toriu and K. Murakami, "Magnetic-multiturn planar coil inductor", *IEEE transactions on magnetics*, Vol. 27, No. 6, pp. 5438–5440, 1991.

18. Poliakine, J., Y. Civet and Y. Perriard, "Design and manufacturing of high inductance planar coils for small scale sensing applications", *Procedia Engineering*, Vol. 168, pp. 1127–1130, 2016.

19. Quinn, C., K. Rinne, T. O'Donnell, M. Duffy and C. Mathuna, "A review of planar magnetic techniques and technologies", *APEC 2001. Sixteenth Annual IEEE Applied Power Electronics Conference and Exposition (Cat. No. 01CH37181)*, Vol. 2, pp. 1175–1183, IEEE, 2001.

20. Faria, A., L. Marques, C. Ferreira, F. Alves and J. Cabral, "A Fast and Precise Tool for Multi-Layer Planar Coil Self-Inductance Calculation", *Sensors*, Vol. 21, No. 14, p. 4864, 2021.

21. Wang, H., M. Totaro, S. Veerapandian, M. Ilyas, M. Kong, U. Jeong and L. Beccai, "Folding and Bending Planar Coils for Highly Precise Soft Angle Sensing", *Advanced Materials Technologies*, Vol. 5, No. 11, p. 2000659, 2020.

22. Liyuan, Y., L. Shushu, N. Pingjuan, S. Hao, M. Run and C. Zheng, "Novel square spiral Coil for achieving uniform Distribution of magnetic Field", *IOP Conference Series: Earth and Environmental Science*, Vol. 332, p. 042005, IOP Publishing, 2019.

23. Anandan, N., A. V. Muppala and B. George, "A flexible, planar-coil-based sensor for through-shaft angle sensing", *IEEE Sensors Journal*, Vol. 18, No. 24, pp. 10217–10224, 2018.

24. Aronov, A. and Y. V. Sharvin, "Magnetic flux effects in disordered conductors", *Reviews of Modern Physics*, Vol. 59, No. 3, p. 755, 1987.

25. Charitat, T. and F. Graner, "About the magnetic field of a finite wire", *European journal of physics*, Vol. 24, No. 3, p. 267, 2003.

26. Caparelli, E. and D. Tomasi, "An analytical calculation of the magnetic field using the Biot Savart law", *Revista Brasileira de Ensino de Física*, Vol. 23, No. 3, pp. 284–288, 2001.

27. Holmes, N., T. M. Tierney, J. Leggett, E. Boto, S. Mellor, G. Roberts, R. M. Hill,

V. Shah, G. R. Barnes, M. J. Brookes *et al.*, "Balanced, bi-planar magnetic field and field gradient coils for field compensation in wearable magnetoencephalography", *Scientific reports*, Vol. 9, No. 1, pp. 1–15, 2019.

28. Liaw, D.-J., K.-L. Wang, Y.-C. Huang, K.-R. Lee, J.-Y. Lai and C.-S. Ha, "Advanced polyimide materials: Syntheses, physical properties and applications", *Progress in Polymer Science*, Vol. 37, No. 7, pp. 907–974, 2012.

29. Feger, C., *Advances in polyimide: science and technology*, CRC Press, 1993.

30. Hatipoglu, G. and H. Ürey, "FR4-based electromagnetic energy harvester for wireless sensor nodes", *Smart Materials and Structures*, Vol. 19, No. 1, p. 015022, 2009.

31. Casanova, J. J., Z. N. Low, J. Lin and R. Tseng, "Transmitting coil achieving uniform magnetic field distribution for planar wireless power transfer system", *2009 IEEE Radio and Wireless Symposium*, pp. 530–533, IEEE, 2009.

32. Zhao, L., J. Van Wyk and W. Odendaal, "Planar embedded pick-up coil sensor for power electronic modules", *Nineteenth Annual IEEE Applied Power Electronics Conference and Exposition, 2004. APEC'04.*, Vol. 2, pp. 945–951, IEEE, 2004.

33. Robaina, R., H. T. Alvarado and J. Plaza, "Planar coil-based differential electromagnetic sensor with null-offset", *Sensors and Actuators A: Physical*, Vol. 164, No. 1-2, pp. 15–21, 2010.

34. Liu, J., W. Lin, J. Wu and J. Zeng, "A novel nine-level quadruple boost inverter with inductive-load ability", *IEEE Transactions on Power Electronics*, Vol. 34, No. 5, pp. 4014–4018, 2018.

35. Ali, M. and A. S. Aminu, "Analysis of Darlington pair in distributed amplifier circuit", *IOSR Journal of Electrical and Electronics Engineering*, Vol. 10, No. 2, pp. 77–80, 2015.

36. ElAhl, A. S., M. Fahmi and S. Mohammad, "Quantitative analysis of high frequency performance of modified Darlington pair", *Solid-State Electronics*, Vol. 46, No. 4, pp. 593–595, 2002.

37. Tang, Y. and T. P. Chow, "High gain monolithic 4H-SiC Darlington transistors", *ISPSD'03. 2003 IEEE 15th International Symposium on Power Semiconductor Devices and ICs, 2003. Proceedings.*, pp. 383–386, IEEE, 2003.

38. SUEN, C., "Characteristics of the Darlington composite transistor", *INTERNATIONAL JOURNAL OF ELECTRONICS*, Vol. 24, No. 4, pp. 373–380, 1968.

39. Krishnaswami, S., A. K. Agarwal, C. Capell, J. Richmond, S. H. Ryu, J. W. Palmour, S. Balachandran, T. P. Chow, S. Baynes, B. Geil *et al.*, "1000 V, 30 A SiC bipolar junction transistors and integrated Darlington pairs", *Materials Science Forum*, Vol. 483, pp. 901–904, Trans Tech Publ, 2005.

40. Srivastava, S., B. Pandey, S. N. Tiwari, J. Singh and S. N. Shukla, "Qualitative analysis of mos based darlington pair amplifiers", *Bulletin of Pure & Applied Sciences-Physics*, Vol. 30, No. 2, pp. 195–203, 2011.

41. Halder, T., "Improved Performance Analysis of Clamp Circuits With Flyback Converter", *International Journal of Emerging Technology and Advanced Engineering*, Vol. 2, No. 1, pp. 1–8, 2012.

42. Mohammed, A. A. and S. M. Nafie, "Flyback converter design for low power application", *2015 International conference on computing, control, networking, electronics and embedded systems engineering (ICCNEEE)*, pp. 447–450, IEEE, 2015.

43. Williams, R. K., M. E. Cornell and J. A. Harnden, "MOSFET flyback-diode conduction and dV/dt effects in power ICs in low-voltage motor control applications", *[1991] Proceedings of the 3rd International Symposium on Power Semiconductor Devices and ICs*, pp. 254–257, IEEE, 1991.

44. Holtz, J., P. Lammert and W. Lotzkat, "High-speed drive system with ultrasonic MOSFET PWM inverter and single-chip microprocessor control", *IEEE transactions on industry applications*, , No. 6, pp. 1010–1015, 1987.

45. Qi, H., S. Ganesan, J. Wu, M. Pecht, P. Matkowski and J. Felba, "Effects of printed circuit board materials on lead-free interconnect durability", *Polytronic 2005-5th International Conference on Polymers and Adhesives in Microelectronics and Photonics*, pp. 140–144, IEEE, 2005.

46. Khan, S., "Comparison of the dielectric constant and dissipation factors of non-woven aramid/FR4 and glass/FR4 laminates", *Circuit World*, Vol. 26, No. 2, pp. 33–37, 2000.

APPENDIX A: ADDITIONAL COMPONENTS AND RESULTS

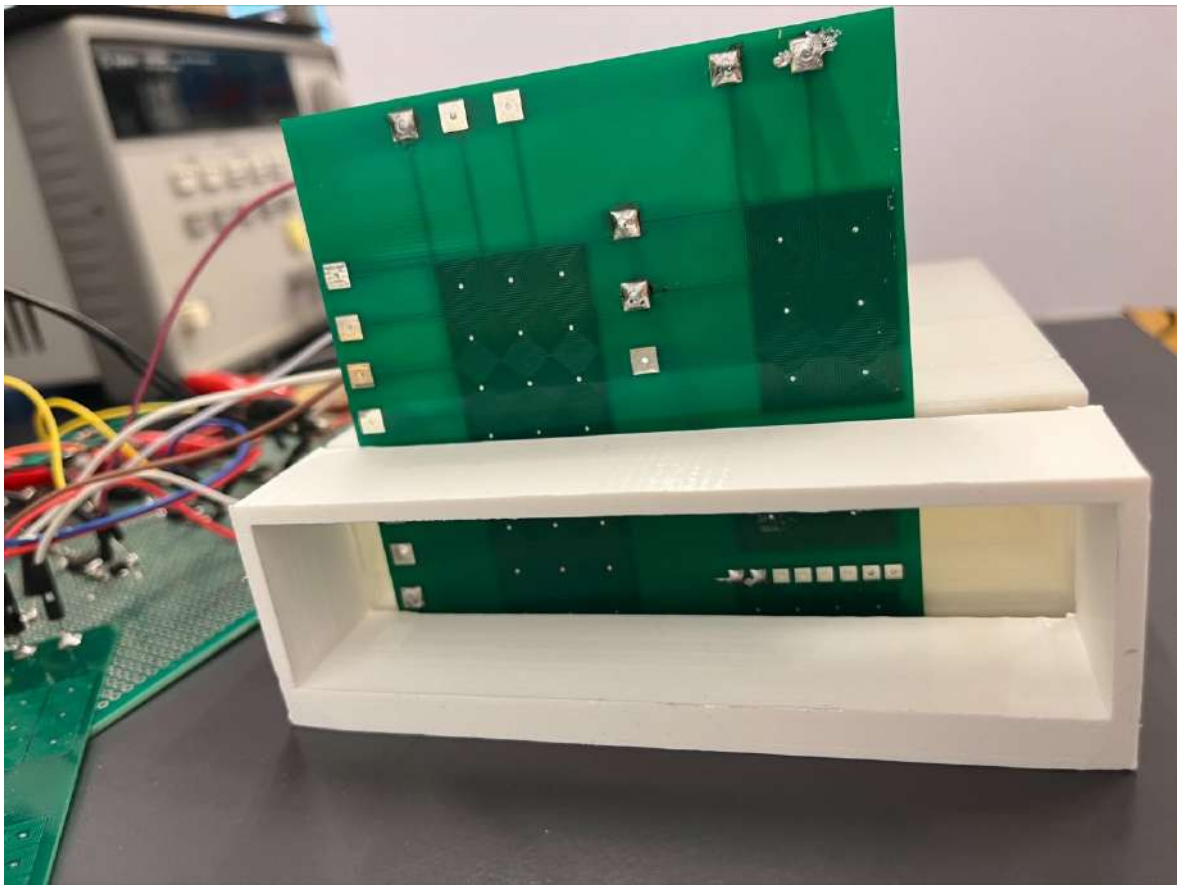

Figure A.1: Three Dimension (3D) Platform holding FR4 planar coil printed circuit board.

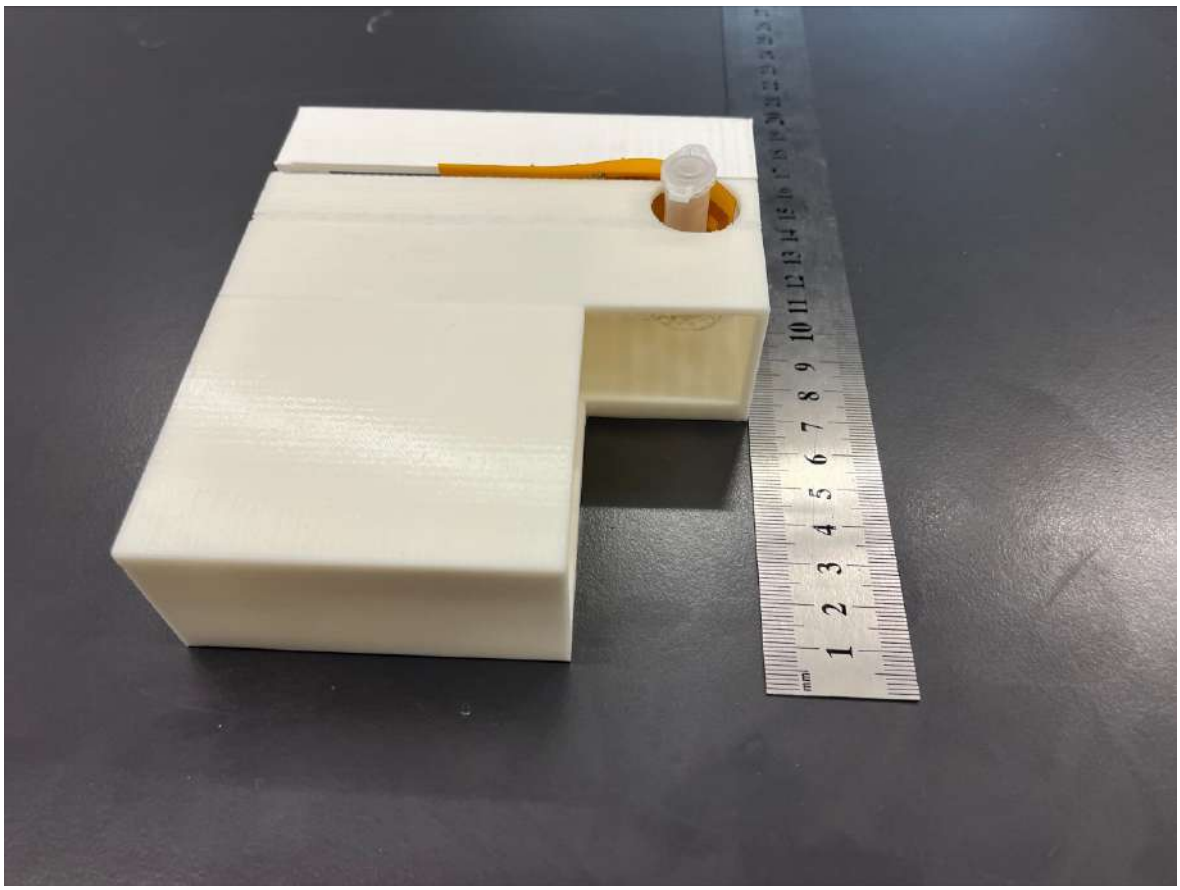

Figure A.2: Three Dimension (3D) Platform holding polyimide planar coil printed circuit board.

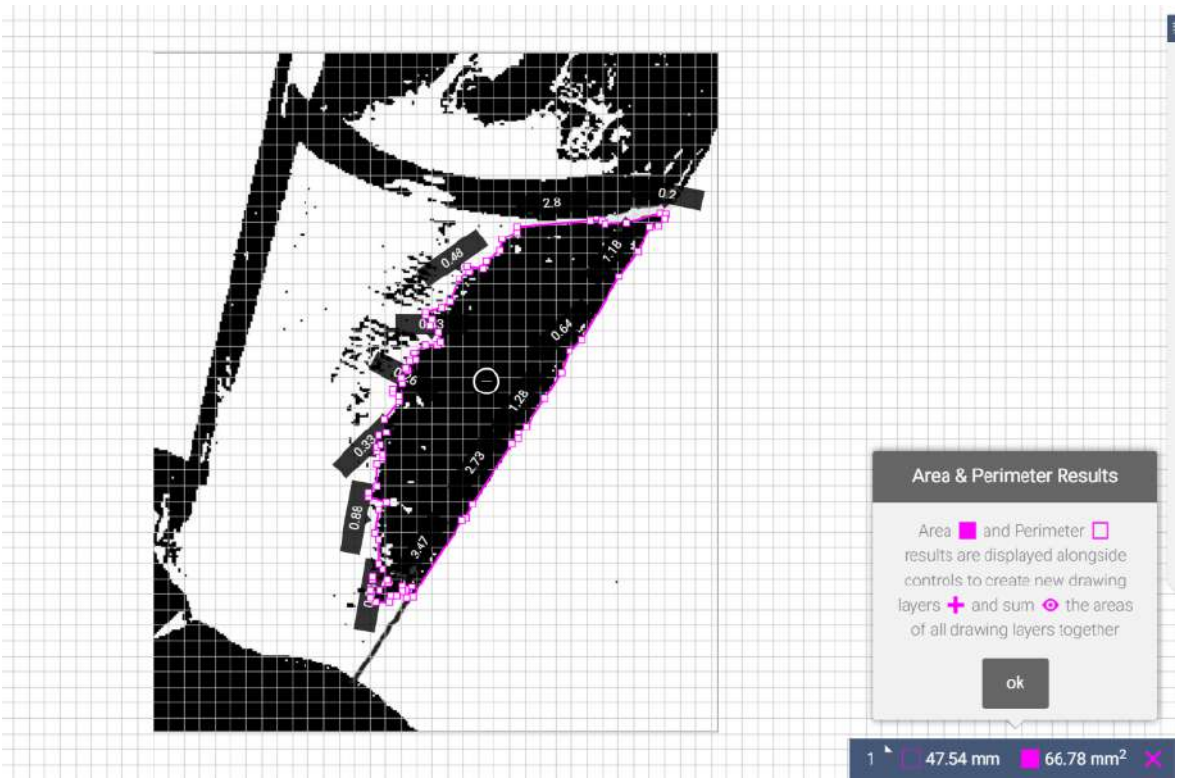

Figure A.3: Close up footage of ImageJ area calculation and results of Polyimide printed circuit board with 35 turned planar coil.

APPENDIX B: DATASHEETS

Surface Mount Rectifiers — *ES1A--ES1J*

FEATURES

Lead-free

- Low cost
- Low leakage
- Low forward voltage drop
- High current capability
- Easily cleaned with Alcohol ,Isopropanol and similar solvents
- The plastic material carries U/L recognition 94V-0

MECHANICAL DATA

- Case: DO-214AC(SMA) molded plastic
- Terminals: Solder able per MIL- STD-202,Method 208
- Polarity: Color band denotes cathode
- Weight: 0.002 ounces,0.064 grams
- Mounting position: Any

Maximum Ratings(@TA = 25°C unless otherwise specified)

Characteristic	Symbol	ES1A	ES1B	ES1C	ES1D	ES1E	ES1G	ES1H	ES1J	UNITS
Device marking		ES1A	ES1B	ES1C	ES1D	ES1E	ES1G	ES1H	ES1J	
Maximum recurrent peak reverse voltage	V_{RRM}	50	100	150	200	300	400	500	600	V
Maximum RMS voltage	V_{RMS}	35	70	105	140	210	280	350	420	V
Maximum DC blocking voltage	V_{DC}	50	100	150	200	300	400	500	600	V
Maximum average forward rectified current @T_A=75℃	$I_{F(AV)}$	1.0								A
Peak forward surge current 8.3ms single half-sine-wave superimposed on rated load @T_J=125℃	I_{FSM}	30								A

Thermal Characteristics

Characteristic	Symbol	ES1A	ES1B	ES1C	ES1D	ES1E	ES1G	ES1H	ES1J	UNITS
Typical junction capacitance (Note2)	C_J	19								p F
Typical thermal resistance	$R_{\theta JA}$	50								℃/W
Operating junction temperature range	T_J	- 55 ---- + 150								℃
Storage temperature range	T_{STG}	- 55 ---- + 150								℃

Electrical Characteristics (@TA = 25°C unless otherwise specified)

Characteristic	Symbol	ES1A	ES1B	ES1C	ES1D	ES1E	ES1G	ES1H	ES1J	UNITS
Maximum instantaneous forward voltage at1.0 A	V_F	0.98				1.25		1.70		V
Maximum reverse current @T_A=25℃	I_R	5.0								μA
at rated DC blocking voltage @T_A=125℃		200								
Maximum Reverse Recovery Time (Note1)	t_{rr}	35								ns

NOTE: 1. Measured with I_F=0.5A, I_R=1A, I_{rr}=0.25A

2. Measured at 1.0MHZ and applied reverse voltage of 4.0VDC

Figure B.1: Datasheet of a flyback diode ES1A.

MOTOROLA
SEMICONDUCTOR TECHNICAL DATA

Order this document by MJD122/D

Complementary Darlington Power Transistors

DPAK For Surface Mount Applications

NPN
MJD122*
PNP
MJD127*

*Motorola Preferred Device

SILICON
POWER TRANSISTORS
8 AMPERES
100 VOLTS
20 WATTS

Designed for general purpose amplifier and low speed switching applications.

- Lead Formed for Surface Mount Applications in Plastic Sleeves (No Suffix)
- Straight Lead Version in Plastic Sleeves ("–1" Suffix)
- Lead Formed Version Available in 16 mm Tape and Reel ("T4" Suffix)
- Surface Mount Replacements for 2N6040–2N6045 Series, TIP120–TIP122 Series, and TIP125–TIP127 Series
- Monolithic Construction With Built–in Base–Emitter Shunt Resistors
- High DC Current Gain — h_{FE} = 2500 (Typ) @ I_C = 4.0 Adc
- Complementary Pairs Simplifies Designs

CASE 369A–13

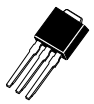

CASE 369–07

MINIMUM PAD SIZES RECOMMENDED FOR SURFACE MOUNTED APPLICATIONS

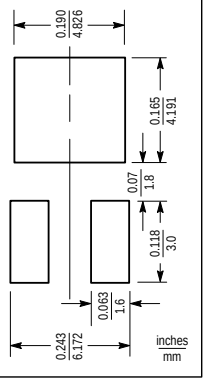

MAXIMUM RATINGS

Rating	Symbol	MJD122 MJD127	Unit
Collector–Emitter Voltage	V_{CEO}	100	Vdc
Collector–Base Voltage	V_{CB}	100	Vdc
Emitter–Base Voltage	V_{EB}	5	Vdc
Collector Current — Continuous Peak	I_C	8 16	Adc
Base Current	I_B	120	mAdc
Total Power Dissipation @ T_C = 25°C Derate above 25°C	P_D	20 0.16	Watts W/°C
Total Power Dissipation* @ T_A = 25°C Derate above 25°C	P_D	1.75 0.014	Watts W/°C
Operating and Storage Junction Temperature Range	T_J, T_{stg}	–65 to +150	°C

THERMAL CHARACTERISTICS

Characteristic	Symbol	Max	Unit
Thermal Resistance, Junction to Case	$R_{\theta JC}$	6.25	°C/W
Thermal Resistance, Junction to Ambient*	$R_{\theta JA}$	71.4	°C/W

ELECTRICAL CHARACTERISTICS (T_C = 25°C unless otherwise noted)

Characteristic	Symbol	Min	Max	Unit
OFF CHARACTERISTICS				
Collector–Emitter Sustaining Voltage (I_C = 30 mAdc, I_B = 0)	$V_{CEO(sus)}$	100	—	Vdc
Collector Cutoff Current (V_{CE} = 50 Vdc, I_B = 0)	I_{CEO}	—	10	µAdc

* These ratings are applicable when surface mounted on the minimum pad sizes recommended.

(continued)

Preferred devices are Motorola recommended choices for future use and best overall value.

REV 1

MOTOROLA

Figure B.2: Datashheet of Darlington Power Transistor MJD122.

Arduino 101 (USA ONLY)
& Genuino 101 (OUTSIDE USA)

Arduino 101 & Genuino 101 are the ideal successor of the UNO, updated with the latest technologies. It recognises gestures, and features a six-axis accelerometer and gyroscope. Control your projects with your phone over Bluetooth connectivity!

Overview

A learning and development board that delivers the performance and low-power consumption of the Intel® Curie™ Module with the simplicity of Arduino at an entry-level price.
It keeps the same robust form factor and peripheral list of the UNO with the addition of onboard Bluetooth LE capabilities and a 6-axis accelerometer/gyro to help you easily expand your creativity into the connected world. .

The module contains two tiny cores, an x86 (Quark) and a 32-bit ARC architecture core, both clocked at 32MHz. The Intel toolchain compiles your Arduino sketches optimally across both cores to accomplish the most demanding tasks.
The Real-Time Operating Systems (RTOS) and framework developed by Intel is scheduled to be open sourced in March 2016. Until then, it's not possible to interface with it directly; only the Arduino core can do it via static mailboxes, so it can only accomplish a predefined list of tasks (interface with PC using USB, program the sketch into flash, expose Bluetooth LE functionality to sketch, perform

Figure B.3: Datasheet of Arduino Uno.